

**Responsive Polymer Composites:
LLDPE/Phenolphthalein Disodium Blends.**

**RESPONSIVE POLYMER COMPOSITES:
LLDPE AND PHENOLPHTHALEIN DISODIUM BLENDS**

By
FADI H. ASFOUR, B.Sc.

A Thesis Submitted to the School of Graduate Studies
in Partial Fulfillment of the Requirements for the
Degree Master of Science

McMaster University

© Copyright by Fadi H. Asfour, August 1997

MASTER OF SCIENCE (1997)
(Chemistry)

MCMASTER UNIVERSITY
Hamilton, Ontario

TITLE: RESPONSIVE POLYMER COMPOSITES: LLDPE AND
PHENOLPHTHALEIN DISODIUM BLENDS

AUTHOR: Fadi H. Asfour, B.Sc.
(Canisius College, Buffalo, NY)

SUPERVISOR: Dr. Harald D. H. Stöver

NUMBER OF PAGES: 84

Abstract:

Responsive polymer composites were developed by incorporating a functional component into a nonpolar amorphous polymer. The response of the polymer composite is the change in color observed upon exposing the composite to different acids. One application could be a device to monitor the diffusion of different acids in different polymers.

The research contained within this thesis deals with an investigation of basic properties of polymer composites. This was accomplished, first through the preparation of a composite of phenolphthalein disodium and Linear Low Density Polyethylene (LLDPE), second, by monitoring the decolorizing process and the aspects that affect it. The investigations included the extrusion parameters, types of acid, acid concentration and indicator concentration, and lastly by quantifying the process through the comparison of empirical diffusion coefficients and corresponding diffusion rates.

This study has shown that decolorization occurs at a fast pace in the presence of acetic acid and slow in the presence of hydrochloric acid. Further as the indicator concentration increases, the decolorization process becomes slower.

Techniques used to monitor the properties were Scanning Electron Microscopy (SEM) micrographs of freeze fractured composites, Differential Scanning Calorimetry (DSC) scans for the starting materials as well as the composites, and photography of the cross-sections of sample composite cylinders.

Acknowledgments

I wish to thank my thesis supervisor, Dr. H.D.H. Stöver, for his guidance, and allowing me to complete my thesis, and letting me discover my own research path.

Also, I would like to also thank Randy S. Frank, Jeff S. Downey and Kimberley D. Gracie for their guidance in writing my thesis.

Many thanks to the following who have contributed to my thesis:

Dr. Pierre Brassard, for understanding diffusion,

Dr. O.E. Hileman, for understanding factorial designed experiments

Our lab group: Dr. Quan Sheng, Jeff (Buck) S. Downey, Randy S. Frank, Wen Hui Li and Pauly Kavalakatt.

Carol Dada and the entire Chemistry Department Staff;

Ontario Center for Materials Research and McMaster University for financial support.

Last, but most certainly not least, I would like to thank my family and friends for their support and understanding.

Table of Contents

Abstract:	iv
Acknowledgments	v
List of Figures	viii
List of Tables	x
Objectives:	1
1.0 Introduction:	2
1.1 Composites:	3
1.1.1 Definition:	3
1.1.2 Blending of incompatible materials:	3
1.1.3 Liquid-liquid systems:	4
1.1.4 Liquid-solid systems:	5
1.2 Polyethylene:	8
1.2.1 General Properties:	8
1.2.2 Morphology:	12
1.2.3 Characterization:	13
1.2.4 Polyethylene Composites:	14
1.3 Phenolphthalein:	15
2.0 Experimental:	20
2.1 Materials used:	20
2.2 Synthesis of phenolphthalein disodium salt:	21
2.2.1 Synthesis:	21
2.2.2 Characterization:	22
2.3 Blending of Composites:	22
2.3.1 Blend preparation:	22
2.3.2 Composite extrusion:	22
2.4 Characterization:	24
2.5 Decolorization experiments:	24
2.5.1. Setup:	24
2.5.2 Data acquisition and analysis:	24

3.0 Results and Discussion:	26
3.1 Composite:	26
3.1.1 Characterization of the composite:	26
3.1.1.1 Characterization of Phenolphthalein Disodium salt:	26
3.1.1.2 DSC of the Composite:	29
3.1.2 Extrusion of composites:	33
3.1.3 Modification of the composite:	37
3.2 Decolorization:	40
3.2.1 Acids:	41
3.2.2 Acid concentrations:	43
3.2.3 Indicator concentrations:	45
3.3 Diffusion:	52
3.3.1 Diffusion Model:	52
3.3.2 Experimental diffusion coefficients:	56
4.0 Conclusions:	62
5.0 Future Work:	64
6.0 Appendix I: Standard NMR data	66
7.0 Appendix II: Extrusion	69
8.0 References:	72

List of Figures

Figure 1.	Dumbbell model of two solid particulates in a viscous melt.	6
Figure 2.	Schematic of LDPE, LLDPE and HDPE.	9
Figure 3.	Long and short chain formation in LDPE	11
Figure 4.	Schematic of crystalline and amorphous.	12
Figure 5.	Scheme of phenolphthalein acid base equilibria proposed by Berger.	16
Figure 6.	Carbon assignment of phenolphthalein.....	17
Figure 7.	Chemical shift diagram acquired by Berger	17
Figure 8.	Cross-section of the single screw extruder.	23
Figure 9.	Data aquisition	25
Figure 10.	^{13}C NMR of phenolphthalein.....	27
Figure 11.	^{13}C NMR of phenolphthalein disodium salt.	28
Figure 12.	DSC of LLDPE	29
Figure 13.	DSC of 0.1%wt indicator composite.....	30
Figure 14.	DSC of 1.0%wt indicator composite.....	31
Figure 15.	DSC of phenolphthalein disodium salt.	32
Figure 16.	DSC heat/cool cycle of phenolphthalein disodium salt.	32
Figure 17.	DSC of 1:1 ethylene glycol to phenolphthalein disodium salt.	38
Figure 18.	DSC of 1:4 ethylene glycol to phenolphthalein disodium salt.	39
Figure 19.	Picture of the decolorization process.....	40
Figure 20.	Graph of acid comparison.	42
Figure 21.	Diffusion rate at different concentrations of acetic acid.	44
Figure 22.	Diffusion rate at different concentrations of hydrochloric acid.	44

Figure 23.	Diffusion rate in water.	45
Figure 24.	SEM micrograph 0.1%wt indicator composite.	46
Figure 25.	SEM micrograph 10.0%wt indicator composite.	47
Figure 26.	Diffusion rate at different loadings in acetic acid.	49
Figure 27.	Diffusion rate at different loadings in hydrochloric acid.	49
Figure 28.	Diffusion rate at different loadings in water	50
Figure 29.	Decolorization of 0.5%wt indicator composite in a) water, b) hydro- chloric acid and c) acetic acid.	52
Figure 30.	Diagram of diffusion front and plate approximation.	54
Figure 31.	Diagram of acid front.	56
Figure 32.	Graph of diffusion coefficients in acetic acid	60
Figure 33.	Graph of diffusion coefficients in hydrochloric acid.	60
Figure 34.	Graph of diffusion coefficients in water.	61
Figure A-1.	Diagram of melt flow in a single-screw extruder	69

List of Tables

Table 1.	Properties of some typical polyethylenes	10
Table 2.	¹³ C NMR peak assignments for phenolphthalein and phenolphthalein disodium.	26
Table 3.	Variables and their levels for the factorial design.	33
Table 4.	Results of the factorial experiment.	34
Table 5.	Statistical analysis of the effects of extrusion.	36
Table 5.	De and RD for 0.1/AcOH data series.	56
Table 6.	De and RD for 0.1/HCl data series.	57
Table 7.	De and RD for 0.1/H ₂ O data.	57
Table 8.	De and RD for indicator concentration (AcOH) data series.	57
Table 9.	De and RD for indicator concentration (HCl) data series.	58
Table 10.	De and RD for indicator concentration (H ₂ O) data series.	58

Objectives:

The composite decolorizes when exposed to acidic media. The objectives of this study are to explain the process of decolorization. This includes:

- a) studying the effect of different acids, attempting to observe if the composite is selective in terms of acid polarity or acid strength
- b) proposing a diffusion mechanism for the decolorization
- c) exploring the use of these composites to measure diffusion coefficients
- d) exploring its use as long term acid meters.

1.0 Introduction:

Polymer composites are used extensively in such everyday applications as fiber reinforced plastics, tires, wire coatings and paints. These polymer composites can be made to serve specific applications by addition of functional components. These materials are termed functional composites.

An example of a functional composite is polyethylene/starch¹⁻³ which was used to monitor water sorption. Similarly the basic concept of this study involves a functional component within a polymer matrix, which was used to investigate the diffusion of acids into a polymer matrix. The production of this composite required that 1) the functional component will visually indicate the presence of an acidic environment by a change in color and 2) the polymer matrix will sustain the functional component, on a permanent basis, while at the same time allowing the slow diffusion of an acid.

To date, blends of phenolphthalein³⁹ and polyethylene⁴⁰ have not been prepared. The fact that these components are well understood individually makes them ideal candidates for a functional composite.

Phenolphthalein disodium salt is an indicator whose color is dark purple and when exposed to acidic conditions turns colorless. It is the existence of this distinct color change that enables the use of the salt for studies of acid diffusion within a matrix.

1.1 Composites:

1.1.1 Definition:

A composite is a material comprised of two or more components, where the properties of the mixture differ from the sum of the individual properties. This concept has been termed synergism. Composites are usually heterophase materials such as plywood or corrugated paper.⁴ Structural composites find use in a variety of areas ranging from aircraft and automobile components to athletic equipment. A composite material must meet the following conditions:⁵

1. A physical blending of the components
2. It consists of two or more physically and/or chemically distinct phases
3. It has characteristics not exhibited by the components in isolation.

Often the components of composites are immiscible and hence a section dealing with this issue is appropriate.

1.1.2 Blending of incompatible materials:

The majority of polymers are incompatible⁴⁰ with each other, which makes it difficult to prepare molecular level polymer blends. Yet polymer alloys and blends represent a major area of research in the plastics industry today. The main reasons for this interest are as follows:

1. The end product can exhibit a high degree of synergism compared to the original components; e.g. polypropylene/polyethylene blends
2. Produce a material at low cost with similar properties to more expensive analogs
3. It can be a viable route for recycling plastics.

There are two key variables that must be dealt with when preparing polymer composites: i) Control of the interfacial chemistry and ii) control of the morphology.

Interfacial interactions:

In some cases it is a requirement for polymer composites to have homogeneous compositions, where the properties are the same throughout the material. This may be achieved through the use of compatibilizing agents. Compatibilization is a process where the interfacial adhesion between the two components is improved by using compounds which contain segments that can chemically or physically interact with the components of the blend. An example of compatibilizing agents are block copolymers that are added⁶⁻⁹ or are created in-situ while processing polymer blends.^{10,11}

Morphology:

Controlling the morphology of the material, means controlling the dispersive behavior of the minor component of the composite. In doing this there are several basic parameters that must be considered:

1. Viscosity and elasticity ratios (liquid-liquid systems)
2. Interfacial tension (liquid-solid and liquid-liquid systems)
3. Shear Stress (liquid-solid and liquid-liquid systems)

1.1.3 Liquid-liquid systems:

According to Willis *et. al.*¹³ the most significant factor in liquid-liquid systems (polymer melts) is the viscosity. Let liquid B be dispersed as a droplet in liquid A and the viscosity ratio be defined as the ratio of the viscosity of liquid A to the viscosity of liquid B. At high viscosity ratios the droplet will burst when the two components are mixed, while at low viscosity ratios the droplet is deformed but does not burst. This indicates that the dispersion of liquid B will be the greatest when the viscosity ratio is high. According to Grace¹² the study of the aforementioned phenomenon has been extensively investigated.

The deformation of a spherical liquid droplet in a homogenous flow field of another liquid was studied in the classical work G. I. Taylor on emulsions.¹⁴ Taylor showed that for simple shear flow, a case in which interfacial tension dominates, the drop would deform into a spheroid with its major axis at a 45° angle to the flow, whereas for the viscosity dominated case it would deform into a spheroid with its major axis approaching the direction of the flow.

Interfacial tension plays as much a role in morphology as it does in the compatibilization. It must be noted that the phase size and the size distribution decreases with the percentage of compatibilizing agent. Willis and Favis¹³ have studied the effect in detail for polyamide/polyolefin blends. Here they reported a rapid drop followed by little change in the phase size with interfacial modifier. This is analogous to the effect found with surfactants in an oil/water emulsion, where at a critical value there is no longer a gain in compatibilization.⁴¹

1.1.4 Liquid-solid systems:

The majority of plastic products produced are mixtures of the basic polymer with a variety of additives such as pigments, lubricants, stabilizers, cross-linking agents and others. All the additives are incorporated into the polymer blend prior to shaping, either during a special postreactor processing step before pelletizing or just before the shaping operation in conjunction with the other elementary steps.

The processing of these mixtures is achieved by dispersive mixing of polymer. This is a process that involves the rupture of clumps and agglomerates of solid particles such as pigments and carbon black in a deforming viscous liquid. This is accomplished by forcing the mixture to pass in high shear zones generated in narrow clearances such as the gap

between the rolls of a roll-mill or in the clearance between the blades and the shell in internal mixers.

Following Bolen and Colwell,¹⁵ it is assumed that the agglomerates break when internal stresses, induced by viscous drag on the particles, exceed a certain threshold value. In this model, the forces are assumed to act on a single agglomerate in the form of a rigid dumbbell. This dumbbell consists of two unequal beads of radii r_1 and r_2 , separated by a distance L , in a homogeneous velocity field of an incompressible Newtonian fluid (Figure 1). As a result of the viscous drag on each of the beads, a certain force develops in the connector \mathbf{R} which depends on the magnitude of the viscous drag and the orientation of the dumbbell. When these forces exceed a certain critical value, which equals the attractive cohesive forces, the beads break apart. The mathematical formulation of this problem was proposed and solved in detail by Bird *et. al.*¹⁶ They showed that the solution was adopted with two minor modifications: i) terms due to Brownian motion, which are irrelevant on this scale, are neglected and ii) the bead radii are assumed to be unequal.

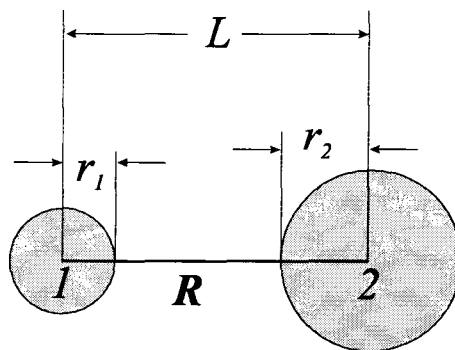


Figure 1. Dumbbell model of two solid particulates in a viscous melt.

It is then assumed that the presence of the dumbbell did not alter the flow field of the liquid in the neighborhood of the dumbbell (i.e. no drift) and the flow is homogenous,

making the rate of deformation the same at all points. For each bead of the dumbbell an equation of motion can be written indicating that mass-time-acceleration equals the sum of forces acting on it. This indicated that the force in the connector is proportional to the harmonic mean of the viscous drags on the beads which depends on the flow field, the orientation of the dumbbell and its size.

This shows that mixer designs should incorporate high shear zones and ensure that all fluid particles pass through the high shear zone repeatedly. Among all mixing operations dispersive mixing is probably the most difficult and costly, therefore it is common practice to prepare master batches which are mixtures containing a high proportion of given additives. For example, in preparing mixtures of polyethylene with carbon black, a superconcentrate containing about 50% carbon black is prepared, then diluted in an internal mixer to 25%, and once more diluted to the final low concentration in a processing extruder. The high intensity deagglomeration operation takes place in the superconcentrate. The dilution of the master batch is a simple extensive mixing operation. Hence by preparing the master batch the difficult and costly dispersive mixing procedure has to be applied to only a small fraction of the final product. Moreover, it is easier to break up clumps and agglomerates at high concentration levels because the high viscosity of the system leads to high local shear stresses and the high concentration facilitates agglomerate breakup by particle interactions. Finally, dilution of master batches makes it easier to maintain uniform product quality than when using a direct mixing process. The color of the product, for example, depends on whether the pigment particles are deagglomerated and by direct mixing this would be more difficult to achieve on a uniform level, than by diluting master batches. Yet the preparation of good master batches is not a simple task and sometimes special precautions must be taken to ensure good dispersion. In dispersing finely divided powders with large surface

areas it is sometimes necessary to wet the surface. For example, water may be added to carbon black before dispersing it in polyethylene.

1.2 Polyethylene:

For this study, the polymer of choice should have the following features: 1) that the polymer be a nonpolar matrix, and 2) its behavior be well understood. One of the polymers that satisfy these aspects is LLDPE, which was chosen for this study.

1.2.1 General Properties:

Polyethylene (PE) is an alkyl chain, containing no pendant groups. Depending on the commercial uses it contains either long, short or no branches; where the degree of crystallinity and the physical properties change according to the average length, of the branches and the degree of branching along the polymer chain.

There are three types of polyethylene (see Figure 5), i) low density polyethylene (LDPE), ii) linear low density polyethylene (LLDPE) and iii) high density polyethylene (HDPE). LDPE has a random distribution of long chain branches along the polymer chain. The polymers usually have a moderately broad molecular mass distribution. LLDPE contains branches of uniform length which are randomly distributed along a given chain, the molecular mass distribution of this class is fairly narrow. HDPE contains no branches, on the other hand has very small amounts that may be deliberately added to fit the use of a specific product. For HDPE, the molecular mass distribution is dependent on the catalyst type.

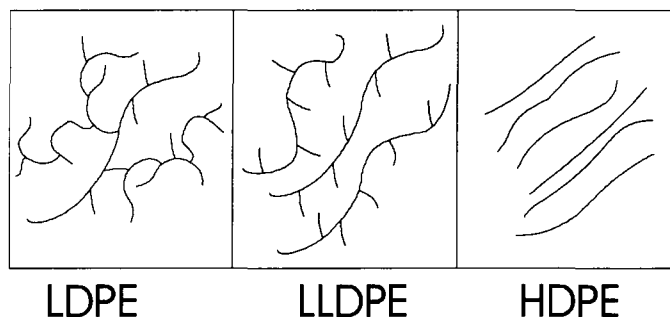


Figure 2. Schematic of LDPE, LLDPE and HDPE.

LDPE and LLDPE are fairly flexible and translucent whitish solids. In the form of films, they have a limp feel with a slight milkiness. HDPE on the other hand, is a white opaque solid that is more rigid and forms films that have an opaque appearance and crisp feel. Polyethylene does not dissolve in any solvent at room temperature, but will dissolve in aromatic and chlorinated hydrocarbons above its melting point ($\sim 140^{\circ}\text{C}$). On cooling these solutions tend to form gels that are difficult to filter.³⁶ Although LDPE and LLDPE do not dissolve at room temperature, they may swell in certain solvents with a deterioration in mechanical strength. In addition to solvents, polyethylene is also susceptible to surface active agents which encourage the formation of cracks in stressed areas over prolonged periods of exposure. This phenomenon is known as environmental stress cracking (ESC) and is believed to be due to the lowering of the crack propagation energy.²⁹

Some properties of typical LDPE, LLDPE and HDPE are listed in the following table.

property	LDPE	HDPE	LLDPE	Method	Standard
Polymer grade	Repsol PE077/A	Hoechst GD-4755	BP LL 0209		
Melt flow index (MFI), g/600s	1.1	1.1	0.85	190°C/2.16 kg	ASTM D 1 238
flight load MFI, g/600s	57,9	50.3	24.8	190°C/21.6 kg	ASTM D1238
Die swell ratio (SR)	1.43	1.46	1.11		
Density, kg/M ³	924.3	961.0	922.0	slow annealed	ASTM D1505
crystallinity, %	40	67	40	DSC	
Temperature of fusion (max.), °C	110	131	122	DSC	
Vicat softening point, OC	93	127	101	5 OC/h	ASTM D1525
Short branches**	23	1.2	26	IR	ASTM D2238
Comonomer		butene	butene	NMR	
Molecular mass M_w	87000*	96000	96000	SEC	
M_n	17,000*	18000	23.000	SEC	
Tensile yield strength, MPa	12.4	26.5	10.3	50 mm/min	ASTM D638
Tensile rupture strength, MPa	12.0	21.1	25.3		
Elongation at rupture, %	653	906	811		
Modulus of elasticity, MPa	240	885	199	flexure	ASTM D790
Impact energy, unnotched, kJ/m ²	74	187	72		ASTM D256
notched, kJ/m ²	61	5	63		ASTM D256
Permittivity at 1 MHz	2.28				ASTM D1531
Loss tangent at 1 MHz	100 X 10 ⁻⁶				ASTM D1531
Volume resistivity, •m	10 ¹⁶				
Dielectric strength, kV/mm	20				

*Not corrected for effects of long branching. ** Number of methyl groups per 1000 carbon atoms.

Table 1. Properties of some typical polyethylenes (data from Repsol Quimica)

In general there are two methods of polymerizing ethylene, either via free radical polymerization or by using transition metal catalysts. LDPE is produced by a free radical polymerization at high temperatures and pressures. The following reaction scheme describes the free radical propagation for long and short chain formation in LDPE:

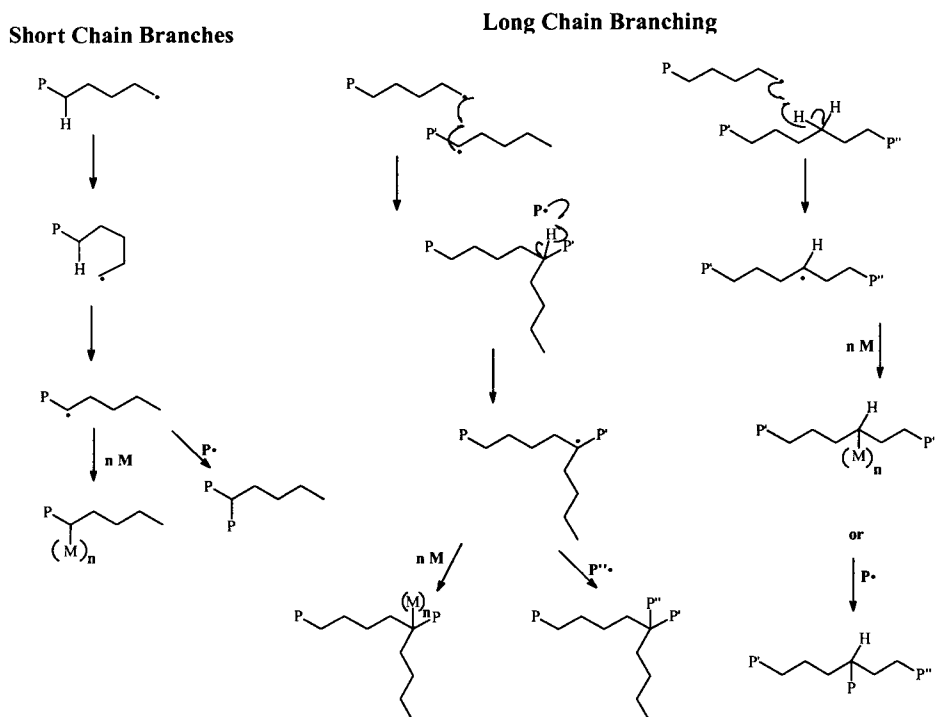


Figure 3. Long and short chain formation in LDPE

Termination is accomplished by the coupling of two propagating polymer chains or by a chain transfer to polymer, solvent or to a chain transfer agent.

LLDPE is manufactured using Ziegler-Natta type transition metal catalysts (eg. $TiCl_3/R_3Al$) in either the solution or gas phase, requiring only moderate temperatures and low pressures (2 atm), making the LLDPE more popular. In order to obtain uniform short chain branches, ethylene is copolymerized with 1-5% of either, 1-butene, 1-pentene, 1-hexene, or 1-octene, allowing the formation of a random copolymer. The amount of comonomer added dictates the characteristics of the final product. The larger the side chain the lower the crystallinity of the material, and the lower the melt viscosity.

HDPE is produced in the same manner as LLDPE, however no comonomer is added, or only very small amounts of 1-butene or 1-hexene are added.

1.2.2 Morphology:

Polyethylene crystallizes in the form of lamellae with a unit cell similar to that of low molecular mass paraffin waxes.³⁰ Chain folding causes the molecular axes to be oriented perpendicular to the longest dimension of the lamella and not parallel. The thickness of the lamellae is determined by the crystallization conditions, the concentration of branches and is typically in the range of 8-20nm. Thicker lamellae are associated with higher melting points and higher overall crystallinity, thus slow cooling from the melt or annealing just below the melting point produces thicker lamellae.

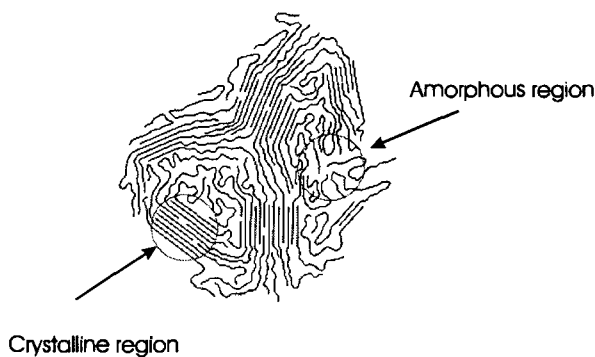


Figure 4. Schematic of crystalline and amorphous.

The side branches are excluded from the crystalline region, as the geometry differs from that of the main chains. Therefore the branches initiate chain folding, which results in thinner lamellae with the branches mainly situated on the chain folds on the surface of the lamellae. However, on rapid cooling these energetically preferred placements may not always occur, and some branches may become incorporated as crystal defects in the crystalline regions. Detailed measurements by solid-state NMR and Raman spectroscopy show that

the categorization into crystalline and amorphous phases is too simplistic. A significant fraction of the polymer is present in the form of an “interfacial” fraction, which is neither amorphous nor crystalline.^{31,32} Under moderately slow cooling conditions, crystallization may be nucleated at a comparatively small number of sites, which then propagate outwards from these centers until the microdomains show a characteristic banded structure under a polarizing optical microscope. The typical milky appearance of polyethylene is due to the light scattering by the microdomains or other, less well defined aggregates of crystallites, not by the crystallites themselves, which are much smaller than the wavelength of light.³³

1.2.3 Characterization:

Polyethylenes are routinely characterized by their density and melt flow index (MFI). The MFI test was originally developed for LDPE to give a measure of the melt characteristics under conditions related to its processing. This is carried out by applying a standard force to a piston and measuring the rate of extrusion (in g/10min) of the polyethylene, through a standard die. The weight-average and number average molecular masses determined by size exclusion chromatography (SEC) or gel permeation chromatography (GPC) for standard PE's are listed in Table 1. LLDPE has a higher number average molecular mass for the same MFI and a narrower molecular mass distribution than does LDPE.

As indicated previously, the crystalline properties are affected by the rate of cooling from the melt and the subsequent thermal history. For the purposes of reproducibility it is important to apply a standard annealing treatment to test samples, such as annealing at 100°C for 5 min followed by slow cooling to room temperature. As with other polymers, polyethylene is viscoelastic in the solid state and the strain produced by applying a stress, is time dependent.

1.2.4 Polyethylene Composites:

There have been many studies on the preparation and characterization of polyethylene composites.^{1,42-45} A few examples are summarized in the following paragraphs.

Sumito *et. al.*⁴², studied the effect of ultrafine particles on the elastic properties of oriented LDPE composites. They mixed fine spherical particles with various diameters (70, 160, and 400 Å and 35μ) with LDPE. These blends were processed and then oriented, to give a hexagonal symmetry. They found that the extremely small particles comparable to the size of the LDPE in the crystalline region exert a considerable reinforcing effect on the oriented polymer matrix.

Kubàt, *et. al.*⁴³ studied the interfacial interactions in HDPE filled with glass spheres (20%vol.). Some of the glass sphere were untreated and some were treated with an azide functional alkoxy silane coupling agent which formed covalent bonds with the polymer. They found that the surface treatment influences the mechanical properties of the composite by improving the interfacial adhesion.

Kalinski *et. al.*⁴⁴ worked on the concept of introducing a liquid layer between the polymer and filler, which led them to LDPE composites containing chalk and oligomers of ethylene oxide. They found that composites containing up to 50% chalk modified with ethylene oxide exhibited typical thermoplastic behavior, i.e., neck formation and plastic deformation, as well as high-impact strength. Based on their data, they suggest that the main action of the ethylene oxide oligomer in the system is to inhibit crack generation and propagation.

Willett¹ and Evangelista *et. al.*⁴⁵ explored the use of polyethylene/starch composites as a device to monitor water sorption and diffusion. The authors of Ref 45 found that the adsorption of water increases in a linear fashion with starch content, while Willett¹ found

that the diffusion coefficients were 2 to 3 orders of magnitude lower than those of water in either LDPE or starch.

The diffusion of acids into a polyethylene matrix is a process yet to be investigated. For this purpose a composite of polyethylene and phenolphthalein salts may prove useful.

1.3 Phenolphthalein:

In 1871 Baeyer¹⁶ described the synthesis of phenolphthalein by condensation of phenol and phthalic anhydride in the presence of anhydrous zinc chloride.²³

Phenolphthalein is commonly used as an indicator, and is also used in the pharmaceutical industry as a laxative.²⁰ It is a white or light yellow crystalline powder, odorless and unstable in air. The glass transition temperature (T_g) is between 75-79°C, with a melting point of 258°C³⁹. It is insoluble in water, but partially soluble in alcohols and etherⁱ and soluble in alkaline solutions. The pH transition interval of phenolphthalein lies between pH 8.2 (colorless) and pH 9.8 (purple). In sodium hydroxide or potassium hydroxide, phenolphthalein forms the corresponding mono, di and tri salts (Figure 5).

Since the discovery of phenolphthalein there has been an intensive debate over the structure as well as the related acid-base equilibria until the 1940s. The current understanding has been arrived at by investigations based on chemical arguments, derivatisation and UV spectroscopy. The debate was laid to rest with ¹H NMR by Ziegler *et.al.*²² and with ¹³C NMR by Berger²³ in 1981. It is now believed that phenolphthalein can engage in the following equilibria: the neutral form **1** is deprotonated to **2**, which opens to **3** to further deprotonate to **4** giving rise to the intensive dark red color above pH 9. In strong alkaline solutions the color fades, and a hydroxylated trianion **5** is formed, Tamura *et. al.*²⁴ measured the absorption

i. Merck Index 11th Ed. 1g/13 ml of alcohol, or /70mls of ether.

spectra of phenolphthalein in solution, and established that the pKa of the first deprotonation was at 9.06 and the second deprotonation pKa of 9.50.

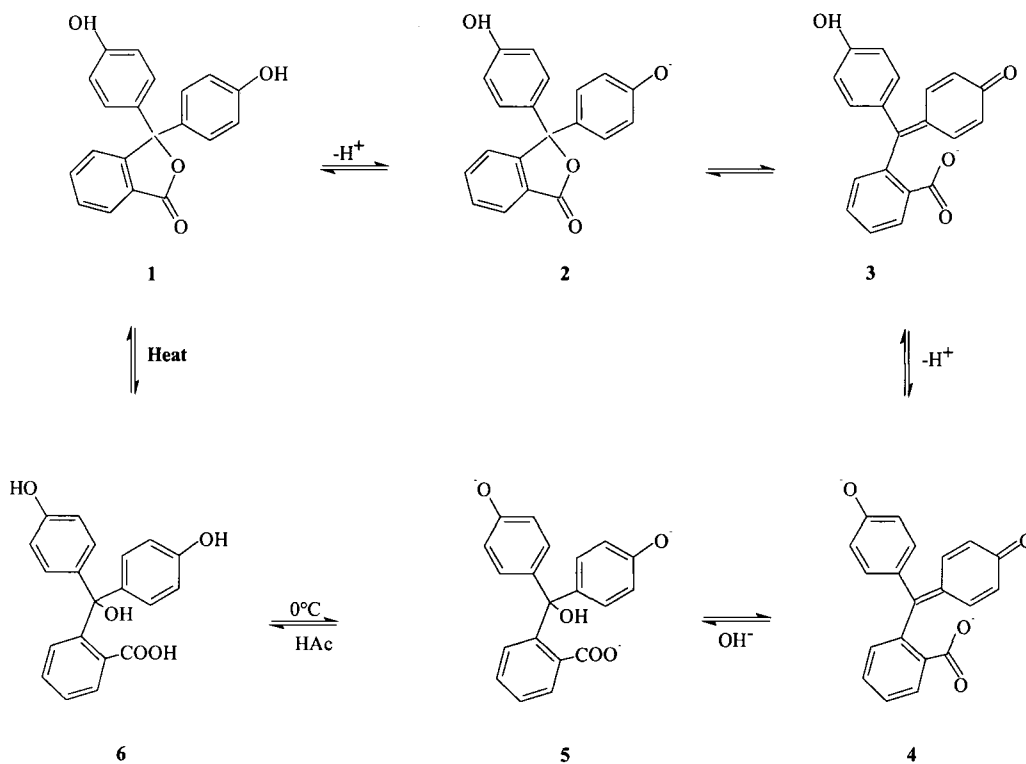


Figure 5. Scheme of phenolphthalein acid base equilibria proposed by Berger.

As reported by Berger, the ^{13}C spectrum²³ (Figure 7) of the neutral compound 1 in DMSO-d_6 gives rise to twelve signals, six of which are from quaternary carbons. The signals were assigned with the help of the proton coupled ^{13}C spectrum. The structure was elucidated by titrating a DMSO solution of phenolphthalein with small amounts of NaOH in H_2O . As depicted in the chemical shift diagram (Figure 7) there are three groups of signals distinguishable by their response to the pH change: C-4 /C-4", C-1 /C-1" and C-3 change

their chemical shifts by about 7-11 ppm, C-1, C-7a, C-4a and C-3 /C-3'' change their chemical shifts by about 1-3ppm and finally C-4, C-5, C-6, C-7 and C-2 /C-2'' remain more or less at their chemical shift position at pH 7.

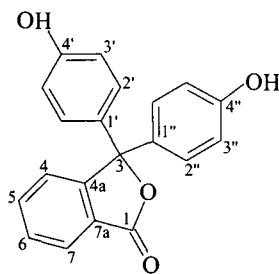


Figure 6. Carbon assignment of phenolphthalein.

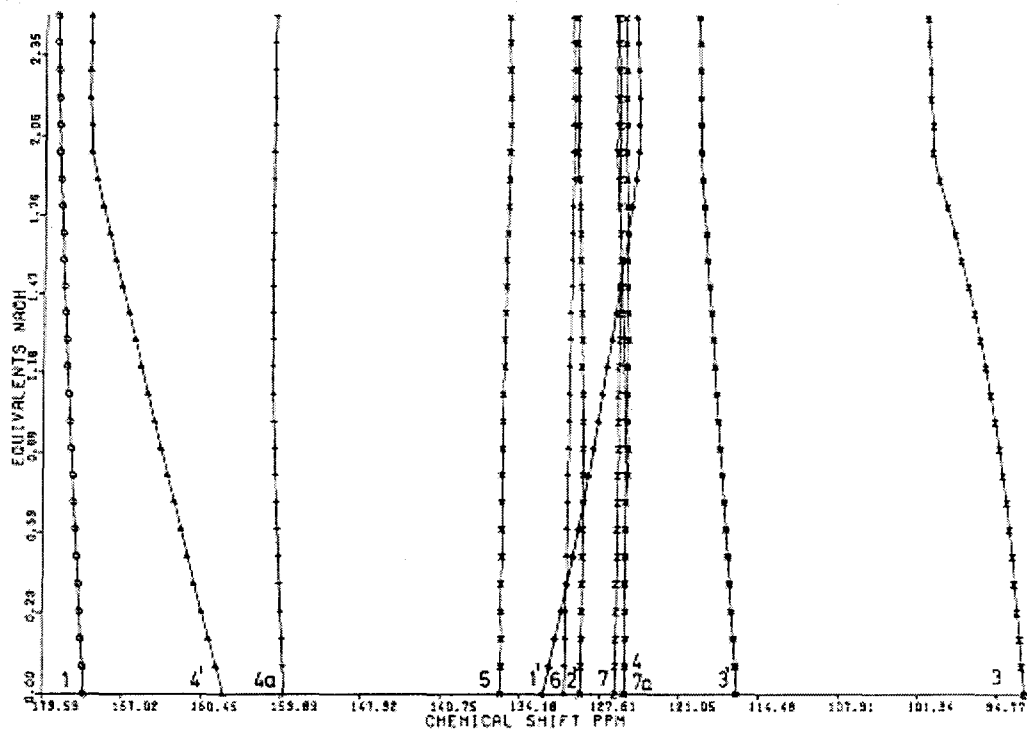


Fig. 1.

Figure 7. Chemical shift diagram acquired by Berger

The strong deshielding of C-4 /C-4" and the shielding of C-1 /C-1" can be explained by a higher electron density in the phenolate anion for C-1 /C-1" and contribution of a CO like structure for C-4 /C-4". However, the deshielding of C-4 /C-4" can be seen in connection with the deshielding of the CO group of carboxylic acid on deprotonation.

As in carboxylic acids, the ring opening and anionization of the lactonoid ring carbon in phenolphthalein, causes a deshielding. The titration diagram does not reveal two distinct deprotonation steps as it was shown earlier²⁶ that the pK_a values of the forms 1 and 3 must be close. As shown in Figure 4, the carbons of phenolphthalein do not change their chemical shift position after two equivalents of base have been added. However, the signals start to disappear at this point and another set of twelve ¹³C signals appear. On the addition of three equivalents of base the ratio of 4 and 5 is about 1:9, and if the solution at this point is made more acidic the conversion of 5 into 4 is completely reversible.

The same set of twelve signals which forms during the titration after more than two equivalents of base have been added, appear in the ¹³C spectrum of phenolphthalein in a strong alkaline medium (5M NaOH). The assignment of these twelve signals was done in the same manner as for the neutral compound. There are several chemical shift changes compared with the neutral compound 1 and the dianion 4, which strongly supports the trianion structure 5 for these solutions.

The chemical shifts of this trianion 5 once formed, do not change by varying the pH of the solution. On back titration of 5 with ice cold acetic acid the dark red color of 4 is not observed, indicating nonreversible behavior.

The phenolphthalein disodium salt $C_{20}H_{12}O_4 \cdot Na_2$ [518-51-4] can be prepared by adding 2 equivalents of sodium hydroxide to phenolphthalein in a methanol solution.²⁷ This provides dark purple crystals that have a gold luster. The material does not have a melting point,

but is shown to decompose at 300°C.²⁸

The salt is soluble in water, methanol and ethanol, but it becomes less soluble as the aliphatic residue (number of carbons) of the alkyl alcohol increases.

2.0 Experimental:

2.1 Materials used:

Phenolphthalein (99.3%), acetic acid (97.0%), hydrochloric acid (36.5-38%), sulfuric acid (95.0-96.0%) and sodium hydroxide (97.0%) were obtained from Bayer Chemicals and were used as received. Methanol (Reagent Grade A.C.S. 99.8%) was obtained from Anachemia. Linear Low Density Polyethylene (LLDPE) was obtained from NOVACOR Chemicals Ltd. as product: SCLAIR® 8710G-UV8D lot # 51755 and was used as is. The following information was taken from the product data sheet supplied by NOVACOR Chemicals Ltd.

SCLAIR® 8107 UV8D, 8107G UV8D

Linear Low Density Polyethylene Rotational Molding

Properties	SI Units	Typical Values ⁱ	ASTM ⁱⁱ
Density	g/cm ³	0.924	D 1505
Melt Index ⁱⁱⁱ	dg/min	5.0	D 1238
Tensile Yield 50mm/min	MPa	10.5	D 638
500mm/min	MPa	11.7	D 638
Elongation 50mm/min	%	850	D 638
500mm/min	%	700	D 638
Flexural Modulus	MPa	345	D 790
Hardness (Shore D)	-	52	D 2240
Softening Point (Vicat)	C	91	D 1525
Low-Temperature Brittleness C point		<-70	D 746
ESCR, F50 ^{iv}	hr	>1,000	D 1693
Molecular Weight: $\overline{M}_w = 89000$			

Processing conditions:

Recommended melt temperature ranges between 170°C - 215°C.

2.2 Synthesis of phenolphthalein disodium salt:

2.2.1 Synthesis:

165 mmol of phenolphthalein was dissolved in 640 ml of methanol, which was calculated from the solubility of phenolphthalein in alcoholsⁱ. 334 mmol of sodium hydroxide was also dissolved in 60 ml of methanol calculated in the same fashion. Complete dissolution of both materials was achieved by heating the solutions. The alkaline solution was then added to the phenolphthalein solution to produce a deep red solution, which was stirred for

i. Typical Values represent average laboratory values and are intended as guides only, not as specifications.

ii. Properties designated have been determined in accordance with the current issues of the specified testing methods. Methods of the American Society for Testing and Materials (ASTM) and used wherever applicable.

iii. Condition 190/2.16

iv. Environmental Stress Crack resistance, Condition A.

v. Merck Index; phenolphthalein: 1g/13 ml of alcohol

10 minutes. The final solution was transferred into a round bottom flask, and the solvent was evaporated on a rotary evaporator, to obtain a deep violet powder with a gold luster in 90% yield. The crystals were dried in a vacuum oven at 80°C overnight to ensure dryness.

2.2.2 Characterization:

The DSC used was a Dupont 2100 differential scanning calorimeter. Prior to each set of experiments on the DSC, a baseline calibration for the experimental range was carried out. Analyses of the composite material was made from 25°C to 250°C at a rate of 10°C/min. Phenolphthalein disodium salt was analyzed as a reversible scan from 50°C to 250°C to 50°C, and the ethylene glycol / phenolphthalein disodium mixtures were scanned from 50°C to 250°C.

Both ^{13}C NMR and ^1H NMR spectra were measured on a Bruker 200MHz spectrometer, using 30mg samples dissolved in methanol- d_6 .

2.3 Blending of Composites:

2.3.1 Blend preparation:

The blends were prepared by mixing phenolphthalein disodium salt with LLDPE in incremental %wt amounts. For most of the experiments 0.1%wt composites phenolphthalein disodium salt was used. The mix was then blended dry for 5 minutes to insure homogeneous mixing.

2.3.2 Composite extrusion:

The extruder used was a Minitruder (Randcastle Inc.) with the following specifications:

1. Single 1/4" screw, 24:1 L/D barrel.

2. Three heated zones with temperature controllers to control within 1°C .
3. Maximum throughput to approximately 120g/hr at maximum speed of 115 RPM controlled by tachometer feedback.

The blend was extruded with the following settings:

rate of mixing: 100 RPM

Temperature setting

Zone 1: 160°C (actual $160 \pm 2^{\circ}\text{C}$)

Zone 2: 160°C (actual $165 \pm 1^{\circ}\text{C}$)

Zone 3: 160°C (actual $160 \pm 2^{\circ}\text{C}$)

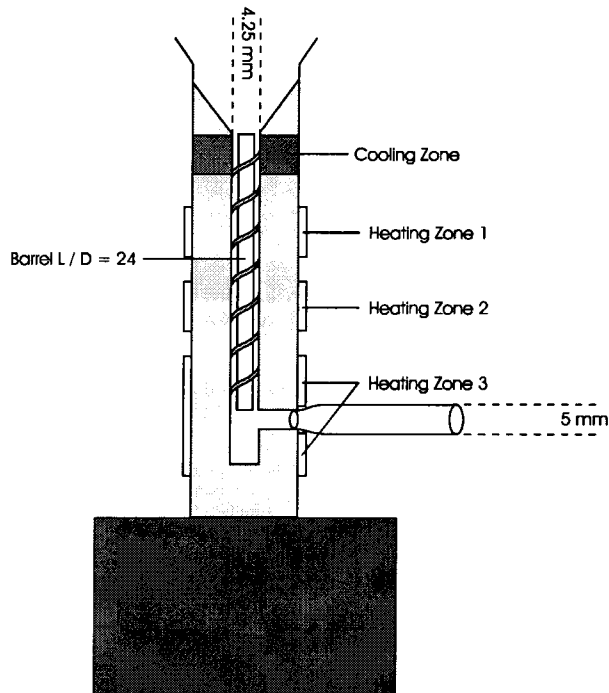


Figure 8. Cross-section of the single screw extruder.

The extrudate was then collected into a modified pasteur pipette as a cylinder mold. The mold was then broken to release the composite cylinder, which was then trimmed to 2.54 cm in length.

2.4 Characterization:

The composites were characterized using DSC to show the melting transition points at 154 °C - 160°C. Environmental Scanning Electron Microscopy (ESEM) was used to examine the shape, size and distribution of the polar indicator within the polymer matrix. Freeze fracture samples were examined with an ESEM equipped with an EDX detector at 15 kV to determine the composition of the embedded material. ESEM: Electroscan 2020 with LaB₆ gun, gaseous secondary electron detectors and a Peltier temperature control Stage and equipped with an EDX analysis.

2.5 Decolorization experiments:

2.5.1. Setup:

Two aspects were investigated, i) the use of various acids namely acetic acid, hydrochloric acid and water. ii) acid concentration: where the acetic acid concentrations used were 17.4 (glacial), 8.7, 1.74, 0.87, 0.3, 0.2M, hydrochloric acid concentrations used were 5.5, 2.7, 1.4, 0.5 and 0.3 M. One experiment was set using 0.1 %wt composites, hydrochloric acid, water and acetic acid. All data points were compiled in triplicate.

The indicator concentration was varied within the composites at levels of 0.1, 0.5, 1.0, 2.0, 5.0, 10.0 %wt. The 0.1 %wt data points were obtained from the previous experiment. The rest of the composites were submerged under water, 5.5M hydrochloric acid, and glacial acetic acid. All data points were obtained in triplicate.

2.5.2 Data acquisition and analysis:

Data points were obtained by destructive sampling of the composites. At each time point, three cylinders were taken, dried with a paper towel and cut in the middle to obtain a cross-section of the composite cylinder. Optical micrograph pictures were taken of each cross-section. The data point for the decolorizing was the difference between the colored radius and the radius of the cylinder (see Figure 9). Multiple measurements were taken for each sample. Camera & Film: Minolta srT200 loaded with KODAK 200 films. The camera was mounted using an accordion and containing a zoom lense.

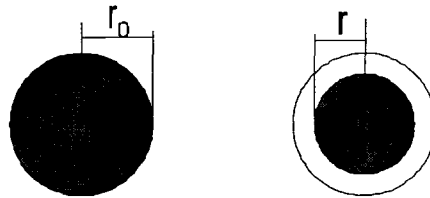


Figure 9. Data acquisition

3.0 Results and Discussion:

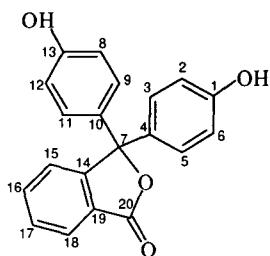
3.1 Composite:

3.1.1 Characterization of the composite:

3.1.1.1 Characterization of Phenolphthalein Disodium salt:

Assignment of the peaks for phenolphthalein were based on two sources: Berger²³ and the Sadtler spectra.ⁱ The assignment of peaks in the phenolphthalein disodium spectra was based on the results of Berger's investigation as well as that of Ziegler *et al.*²² The peaks assigned were in reasonable agreement with those reported.

¹³C peak assignments:



Carbon #	Phenolphthalein (ppm)	Phenolphthalein disodium (ppm)
20	172.01	173.2
1,13	158.8	167.8
14	154.5	155.5
16	135.6	134.9
4,10	133.01	125.88
18	130.4	127.09
3,5,9,11	129.6	129.8
17	126.4	134.9
19	126.2	127.74
15	125.5	126.15
2,6,8,12	116.1	119.10
7	93.8	99.74

Table 2. ¹³C NMR peak assignments for phenolphthalein and phenolphthalein disodium.

i. See appendix for standard spectra.

Figure 10. ¹³C NMR of phenolphthalein.

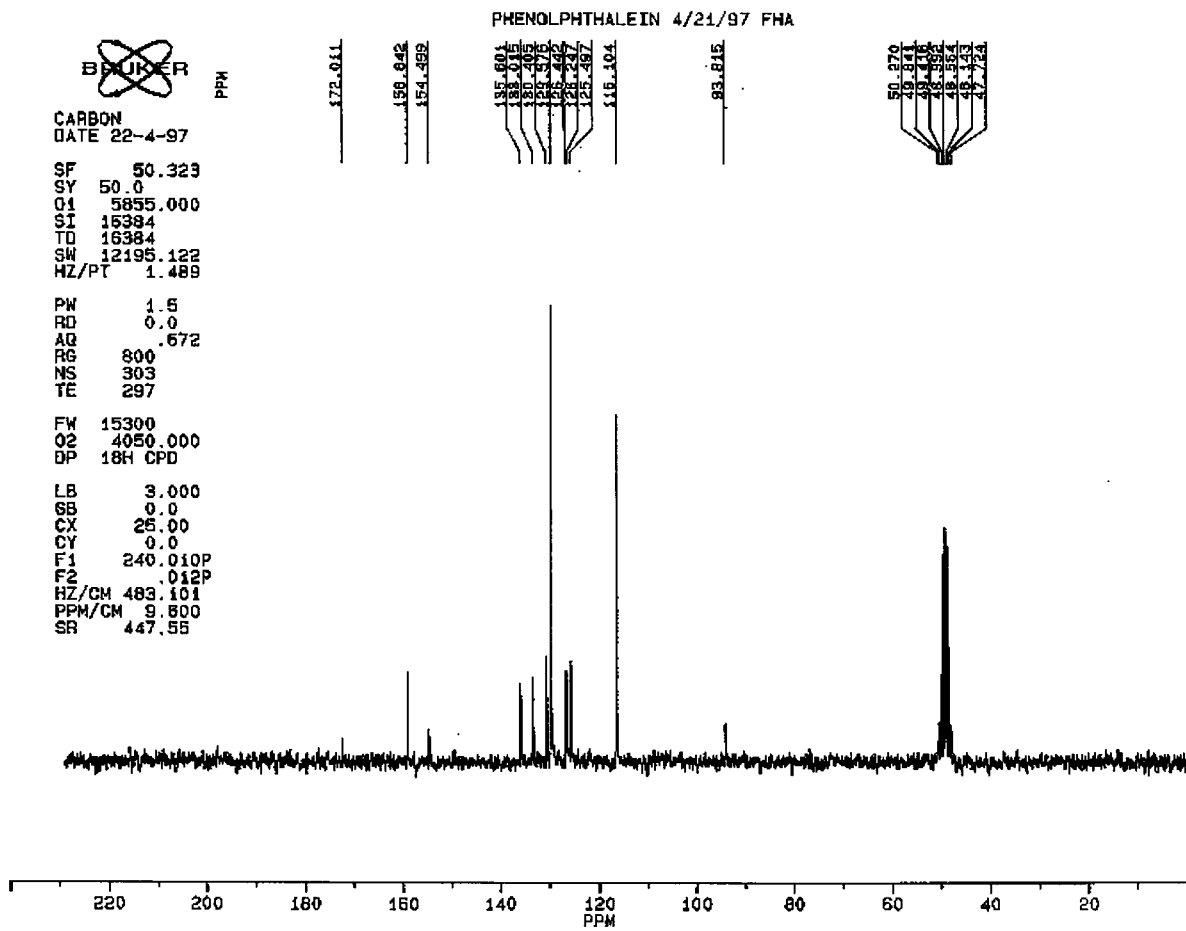
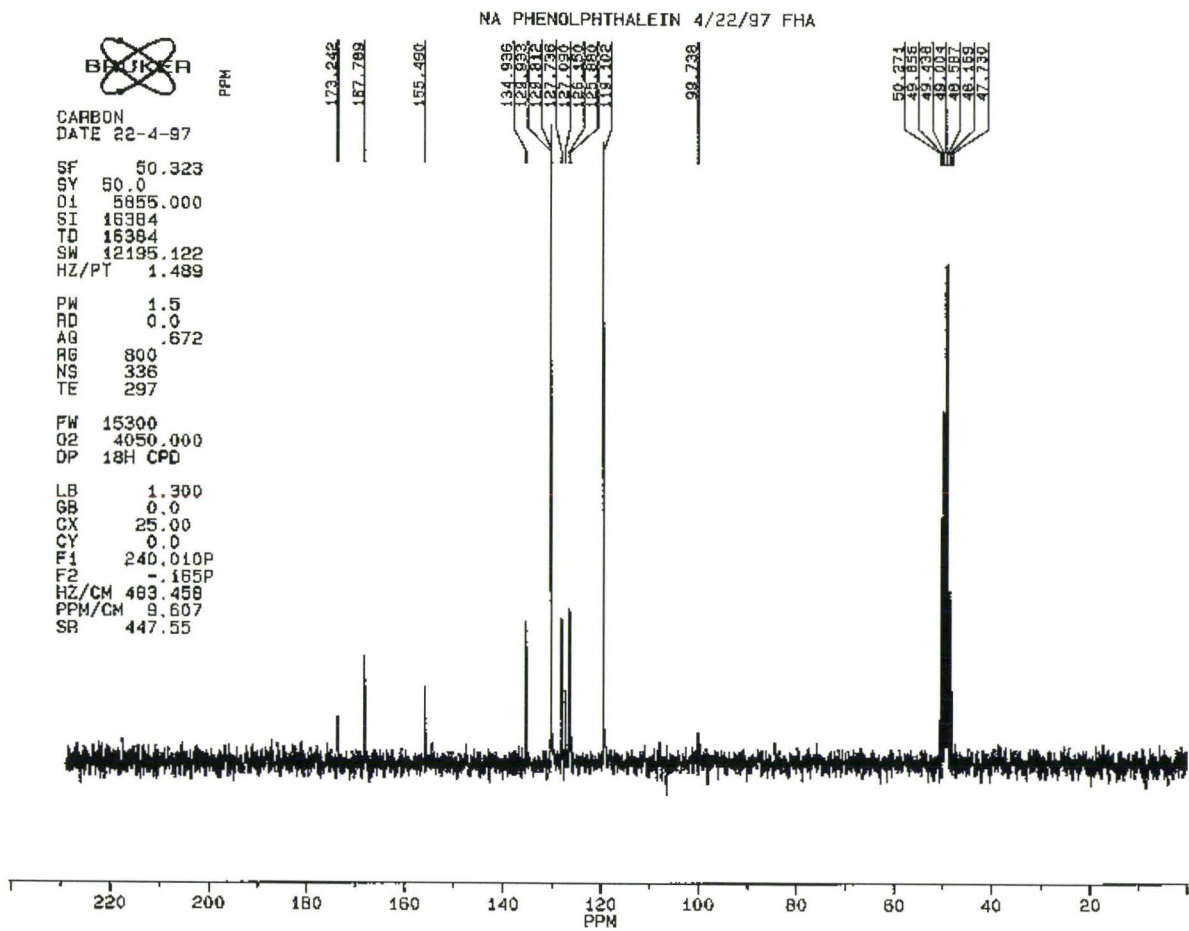


Figure 11. ^{13}C NMR of Phenolphthalein disodium salt.



3.1.1.2 DSC of the Composite:

Differential scanning calorimetry is a useful technique employed to investigate the thermal properties and consequently the structural properties of the material. LLDPE has a softening point at 90°C which is observed in Figure 12, as the onset of the single transition. This transition corresponds to the melting of the material. The DSC scans of the composites at 0.1wt% and 1.0wt% loading showed similar transitions. This can mean one of two things, either the indicator does not melt or that the loading is too small to observe any transitions contributed by the indicator (Figure 13 and 14). At 1.0%wt the melting transition of the polymer occurs at 102°C (Figure 14). Increasing the amount of indicator does not cause a subsequent decrease in the temperature of the melt transition of the polymer.

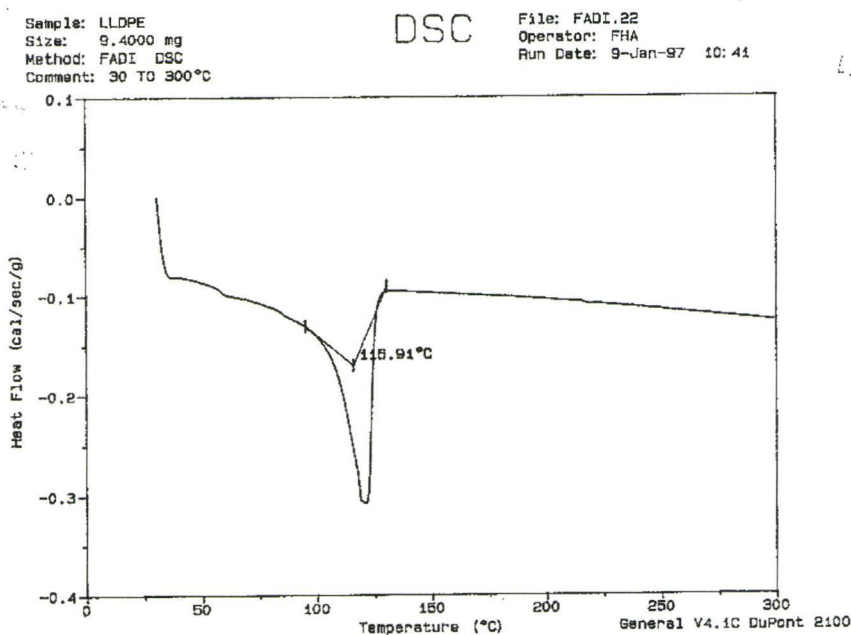


Figure 12. DSC of LLDPE

Sample: 0.1 %NT NAPHPH/LLDPE
Size: 9.5000 mg
Method: FADI DSC
Comment: 30°C TO 300°C

DSC

File: FADI.19
Operator: FHA
Run Date: 8-Jan-97 16:29

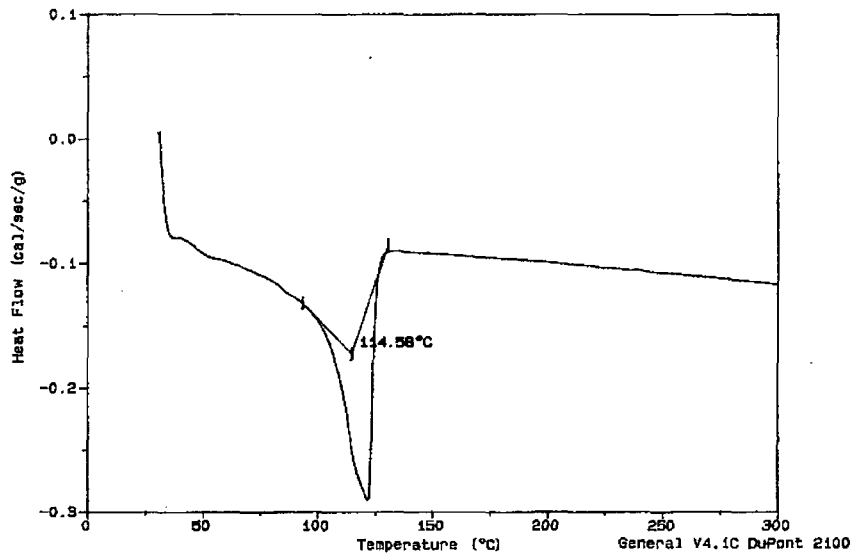


Figure 13. DSC of 0.1%wt indicator composite.

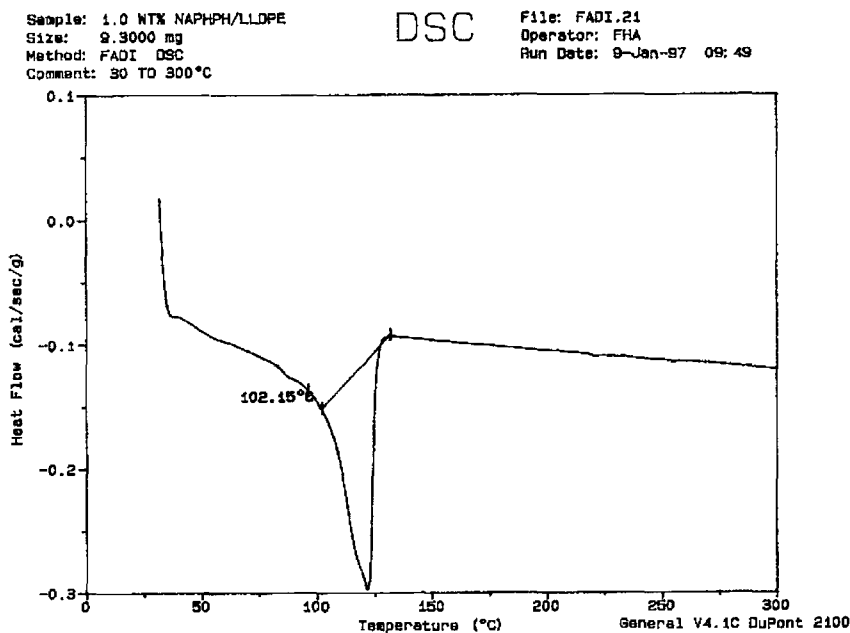


Figure 14. DSC of 1.0%wt indicator composite.

Previous scans of the neat indicator salt showed several broad transitions at around 150°C (Figure 15). To determine whether this was an evolution of volatiles or a structural transition a heat/cool scan was done. Here the sample was heated from 50°C to 250°C and cooled back to 50°C (Figure 16). The transition at 150°C was observed on the heating curve, however it is not observed on the cooling curve. The conclusion can be made that this is not a structural transition but a gas emission. A melting transition is characterized by an intense sharp transition in the thermograms, and this was not observed for phenolphthalein disodium in the DSC scans, rather a melting with decomposition was observed at 315°C in a melting point apparatus. According to the literature there is no melting point for phenolphthalein disodium salt, rather a decomposition is observed at 300°C.²⁸ Phenolphthalein on the other hand has a temperature of vitrification T_g at 75°C and a melting point at 261°C.

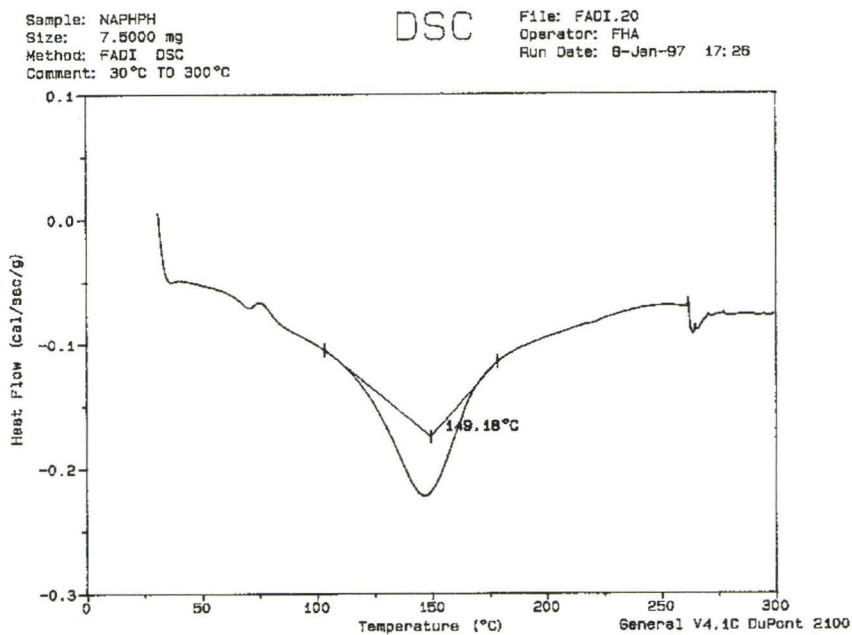


Figure 15. DSC of phenolphthalein disodium salt.

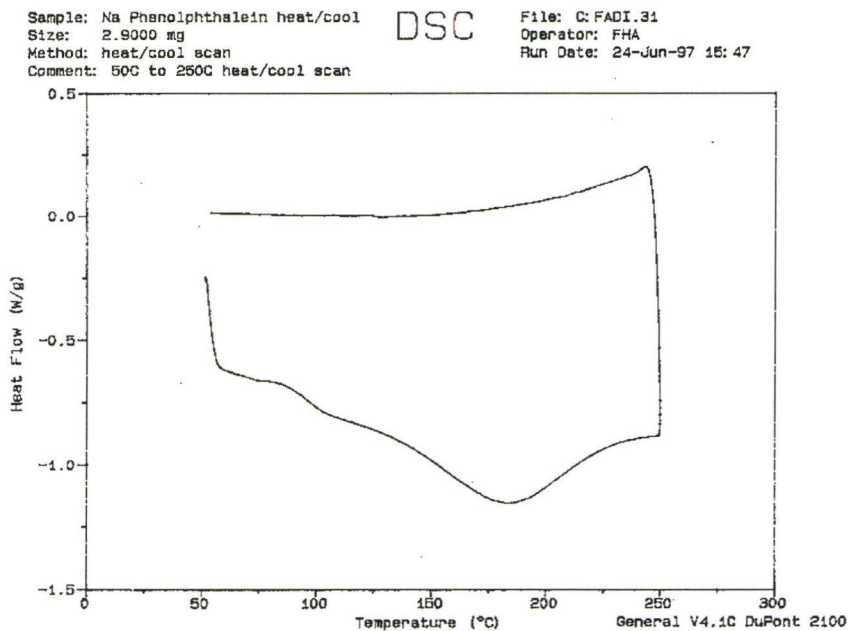


Figure 16. DSC heat/cool cycle of phenolphthalein disodium salt.

3.1.2 Extrusion of composites:

Extrusion parameter effects:

This experiment was used in order to determine the extrusion parameters to use. The experiment was setup using 2^3 factorial design, where 2 represents two levels (high and low) for each variable, and the power of 3 represents three variables. The variables being the indicator concentration, temperature of extrusion and rate of mixing. The high and low levels for each are presented in table 3.

Variable	Low	High
Indicator concentration (C)	0.1%wt	1.0%wt
Temperature (T)	160°C	240°C
Rate of mixing (R)	10 RPM	100 RPM

Table 3. Variables and their levels for the factorial design.

Three samples from each run were submerged in glacial acetic acid and the decolorization was monitored over a period of 7 days.

Table 4 shows the results of the parameter study. The response measured was the time needed to decolorize half the volume of the cylinders ($t_{1/2}$).

Run #	Conditions			Response		
	(%wt) Indicator	(°C) extrusion	(RPM)	Homogenous color	Speckles	<t1/2> (hrs)
1	0.1	160	10	no	yes	—
2	1.0	160	10	yes	no	34.5
3	0.1	240	10	no	yes	—
4	1.0	240	10	yes	yes	25.8
5	0.1	160	100	yes	no	15.9
6	1.0	160	100	yes	no	60.1
7	0.1	240	100	yes	no	20.9
8	1.0	240	100	yes	no	43.8

Table 4. Results of the factorial experiment.

At low indicator loadings and low rates of mixing, the composites were not uniform in color and contained very large clusters which were obvious to the naked eye, indicating that there was no means to measure the decolorization, due to the lack of uniformity in color. The higher rates of mixing, regardless of indicator loading, provided uniformly colored cylinders. Of these, the fastest to decolorize was run #5 which contained 0.1wt% indicator and was extruded at 160°C. The slowest was run #6 which, although was extruded at the same temperature contained a 1.0wt% loading.

The above data indicates that the higher the concentration of indicator the slower the decolorization process and how the distribution is affected by the rate of mixing. Due to the nature of the mixing which is mechanical³⁴, the effect of increasing the rate of mixing results in an increase in the degree of dispersion of the indicator within the polymer matrix. The dispersion is reflected in the size of the indicator domains and in the distribution of these domains.

A statistical analysis³⁸ of the above data yields table 3. The estimates calculated are the difference in the average response at each level of the variable, over all other conditions (equation 1)

$$main\ effect = \overline{y_+} - \overline{y_-} \quad (1)$$

where y_+ is the response at the higher level, and y_- is the response at the lower level. The interaction effects include the two-factor effects and the three-factor effects, which represent combinations of factors that have a significant effect on the measured response. The two-factor effect is described in equation 2, 3 and 4. Let y_n represent the response for run n , then the equations for estimating the two-factor interactions will be:

$$C_{xT} = \frac{y_1 + y_4 + y_5 + y_8}{4} - \frac{y_2 + y_3 + y_6 + y_7}{4} \quad (2)$$

$$C_{xR} = \frac{y_1 + y_3 + y_6 + y_8}{4} - \frac{y_2 + y_4 + y_5 + y_7}{4} \quad (3)$$

$$T_{xR} = \frac{y_1 + y_2 + y_7 + y_8}{4} - \frac{y_3 + y_4 + y_5 + y_6}{4} \quad (4)$$

and the equation for estimating the three-factor effects is:

$$C_{xTxR} = \frac{y_2 + y_3 + y_5 + y_8}{4} - \frac{y_1 + y_4 + y_6 + y_7}{4} \quad (5)$$

Significant factors are selected based on the magnitude of their estimates, which are an indication of the degree of change in the response of the system. However, it must be noted that significant effects due to the two-factor interactions represent a dependence between the two variables. A significant effect due to the three-factor interaction, represents a dependence between all three factors.

The following estimates were calculated based on the time needed to decolorize half the volume of the composite cylinder ($t_{1/2}$). In the cases where no value for $t_{1/2}$ was obtained, zero was assigned for those data points. This introduces an error into the calculations, and indicates that the settings for the low point (0.1%wt) should be increased for the indicator concentration and the rate of mixing in order to obtain a response. As the number of valid responses is reduced from 8 to 6, which reduces the accuracy of the calculations. However, a general sense of the effects of the parameters can still be extracted. Generally, the calculations are adequate if the observed relative standard error is below 5%.

Effect	Estimates	Standard Error
Average	25	3.4
Main effects		
Indicator concentration (C)	32	3.4
Temperature (T)	-5	3.4
Rate of mixing (R)	20	3.4
Two-factor effects		
C x T	-7.5	3.4
C x R	1.7	3.4
T x R	-0.6	3.4
Three-factor effects		
C x T x R	-3	3.4

Table 5. Statistical analysis of the effects of extrusion.

The data indicates that the significant factors effecting the decolorization are i) the indicator concentration and ii) the rate of mixing. Temperature does not play a significant role since the indicator does not melt during the extrusion of the polymer.

The rate of mixing plays a role in homogenizing the composite, since it is a

mechanical mechanism that disperses the indicator within the polymer matrix. Thus the slower the rate of mixing, the lower the shear stress inside the barrel of the extruder, which in turn means the larger the domains of the indicator within the polymer matrix.

Abnormalities would arise throughout the extrusion of the composite cylinders in the form of different color densities that would become more apparent during the decolorization process. The error due to these abnormalities is compensated for by randomly placing the composite cylinders in the sample acid vials. The random sampling and having each measurement performed in triplicate, would minimize this error.

3.1.3 Modification of the composite:

Difficulty in resolving the colored boundary arose at low indicator concentrations which resulted in a very faint cross section. To address this problem, thicker cross sections of the cylinders were taken. The difficulty arises from the poor color dispersion within the matrix. There are two ways of enhancing the dispersion of the indicator are i) either lower its melting point or ii) add a dispersive aid such as a high boiling solvent. In an attempt to lower the melting point of the indicator salt, ethylene glycol (EG) was added as a high boiling solvent (boiling point of 280°C). Figures 17 & 18 are thermograms of 1:1 and 1:4 EG to Phenolphthalein disodium respectively.

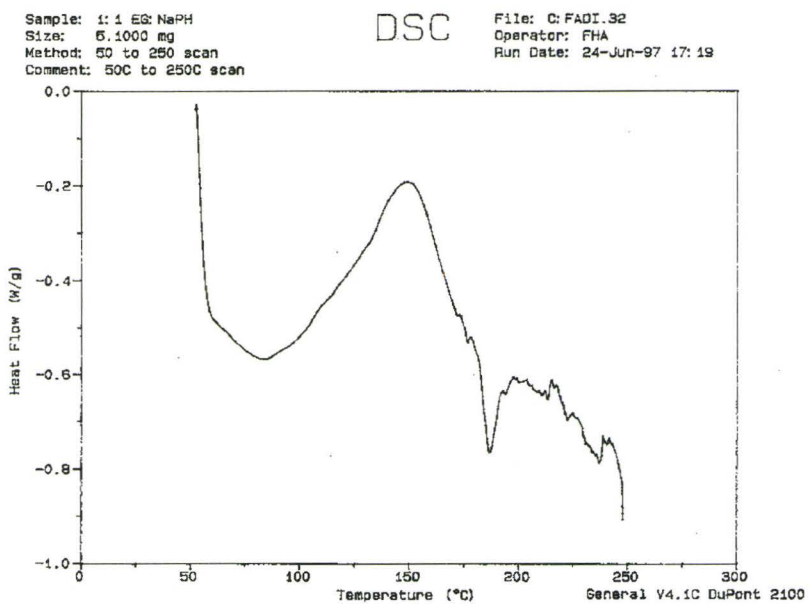


Figure 17. DSC of 1:1 Ethylene Glycol to phenolphthalein disodium salt.

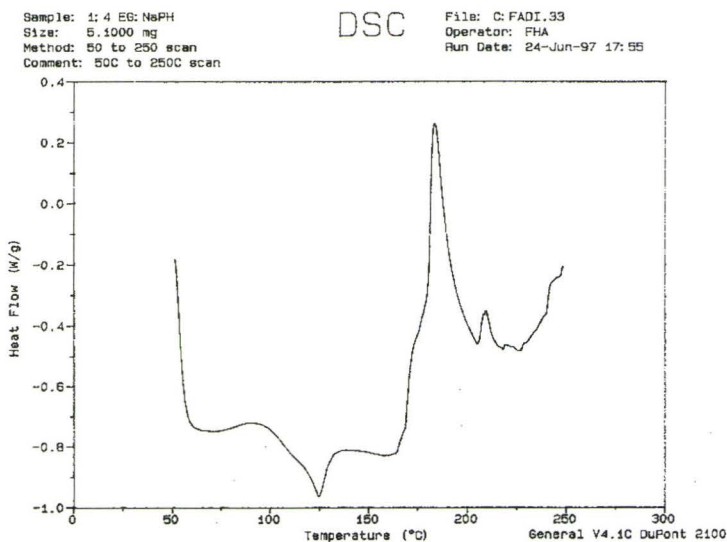


Figure 18. DSC of 1:4 Ethylene glycol to phenolphthalein disodium salt.

The physical appearance of the 1:1 mixture of EG/Phenolphthalein disodium was that of a sticky, viscous paste, while the 1:4 mixture was a sticky solid cluster. No melting transitions were observed in either case. It was observed that the hermetic pans used expanded and in some case ruptured due to the volatile emission from the indicator salt. It is speculated that the water vapour trapped in the pan may have caused the rupture. This was recorded on the thermograms as a large positive heat flow at temperatures that differed for each mixture, it is thought that these transitions represent dissolution endotherms. For the 1:1 mixture this transition was observed at 150°C and for the 1:4 mixture it was observed at ~190°C. When a solvent is added to a solid it normally acts to lower the melting point by lowering the vapor pressure of that material. This does not relate for the decomposition point of the material. Nevertheless, this phenomenon implies that if a 1:1 mixture of ethylene glycol and phenolphthalein disodium are added to the composite batch the resulting composite would contain finely dispersed polar domains. This also means that the mechanism of mixing within the extruder will change from that of a solid particulate in a viscous liquid to that of two viscous liquids.

3.2 Decolorization:

The decolorizing process occurs when an acid diffuses into the matrix of the composite. Upon diffusion, the acid encounters an indicator molecule, protonation of the indicator occurs which is rendered colorless, so the color boundary represents the diffusional front of the acid.

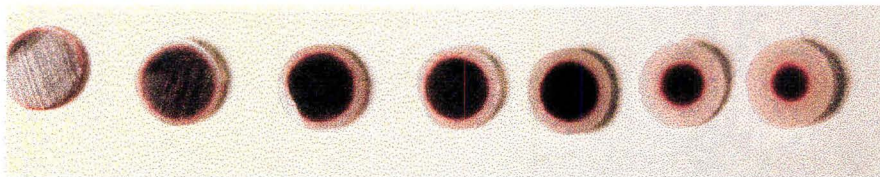


Figure 19. *Picture of the decolorization process.*

There are three cases of diffusion in polymers: i) Fickian or Case I, ii) Non-Fickian or anomalous and iii) Case II diffusion. In Fickian diffusion the rate of diffusion (R_d) is less than the rate of segmental chain motion of the polymer (R_s) and $n=1/2$. In Non-Fickian diffusion, R_d is approximately equal to R_s and $1/2 < n < 1$. In Case II diffusion, R_d is greater than R_s and $n=1$. The value of n is constant for each case where a plot of the distance diffused versus t^n will be linear. Ideally, pure Fickian diffusion applies to completely amorphous polymers and the diffusion coefficient is independent of concentration. While Case II diffusion applies to crystalline polymers or polymers below the glass transition temperature.

It has been observed both theoretically⁴⁶ and experimentally⁴⁷⁻⁴⁹ that polymers such as polyethylene exhibit Fickian behavior and diffusion is concentration dependent. Such systems can be described mathematically by equation 6.⁴⁸

$$\left(\frac{\delta x}{\delta t} \right)_c = f(D, C) t^{1/2} \quad (6)$$

which relates distance diffused to the square root of time. This can be applied to this system as a change in the colored radii ($r-r_0$) with $t^{1/2}$, where r is the colored radius and r_0 is the original radius of the composite cylinder.

3.2.1 Acids:

The following experiment was designed to compare the diffusion rates of different acids. Acetic acid was chosen to represent the weak organic protic acids and Hydrochloric acid to represent strong polar acids and water as a control. Theoretically, the organic protic acids should cause a faster decolorization than the polar acid or water, based on a matrix compatibility argument. It is possible that the diffusing species is the associated acid molecule, rather than the proton itself. The following figure is a comparison of the diffusion rate of glacial acetic acid, hydrochloric acid (5.5M) and water.

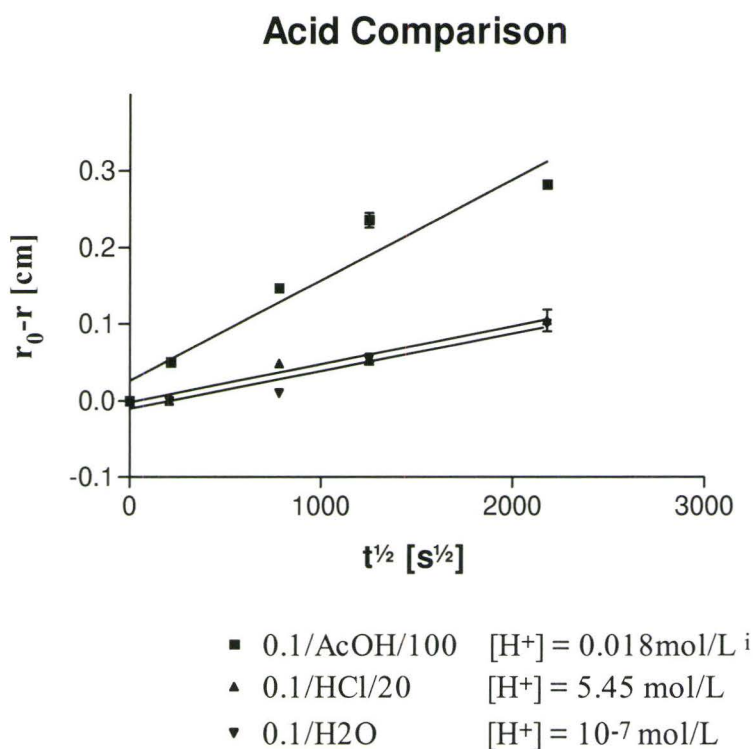


Figure 20. Graph of Acid comparison.ⁱⁱ

When changing the type of acid, there are two parameters that should effect the diffusion rate which is related to the apparant decolorizing rate: i) the acid strength, which relates the concentration of protons to the rate of decolorization of the composite, and ii) the compatibility of the acid with the polarity of the polymer matrix. However these two parameters cannot be distinguished from this graph. The relatively high diffusion rate of glacial acetic acid may be due to the greater affinity of acetic acid to the polymer matrix as opposed to ionic species diffusing in.

ⁱ. Based on pKa of 4.7 in water

ⁱⁱ. Legend: Indicator concentration/Acid/Acid concentration %v/v. This notation will be used throughout this thesis for the graphs

3.2.2 Acid concentrations:

As in the previous section, this experiment is designed to demonstrate the effect of acid concentration. Intuitively, the higher the acid concentration the faster the decolorizing process will occur. However, it may be possible that another aspect can be derived from this data: the species diffusing into the polymer matrix.

In the case of acetic acid (Figure 21), there is a substantial difference between the decolorizing rates at different acid concentrations. It can be stated that the more acid molecules there are, the more indicator molecules can be protonated. However, the graphs acetic acid have greater rates, compared to the graphs observed for hydrochloric acid and water. This leads to the assumption that it is not the acidic proton ($\text{H}^+/\text{H}_3\text{O}^+$) that diffuses in but the associated species of the acidic proton and its conjugate base. Since the degree of dissociation of acetic acid is lower than that of the hydrochloric acid, as it is a weak acid. This suggests that the mechanism of decolorization involves the diffusion of the associated acid into the polymer matrix. Once it reaches the polar indicator domain, the acid dissociates to protonate the indicator.

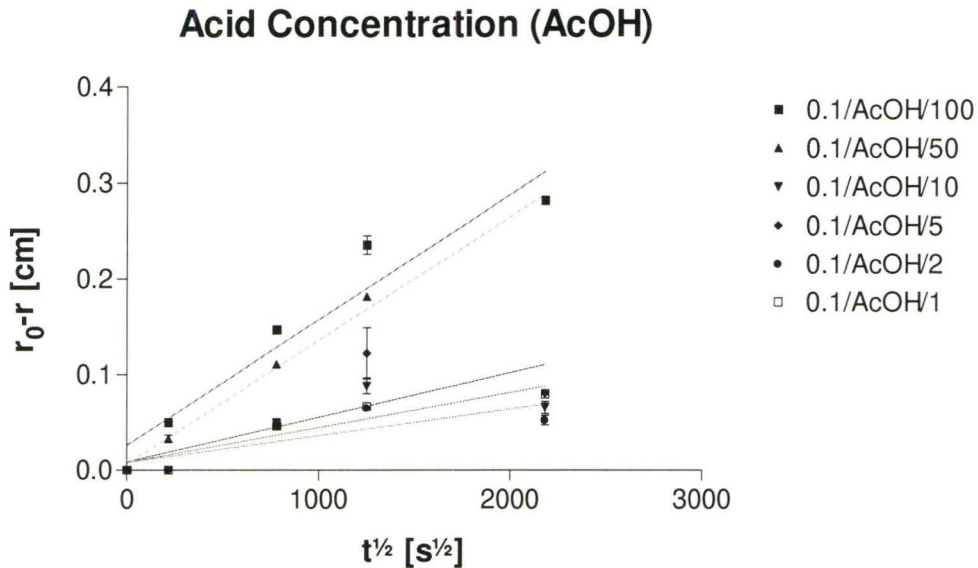


Figure 21. Diffusion rate at different concentrations of acetic acid.

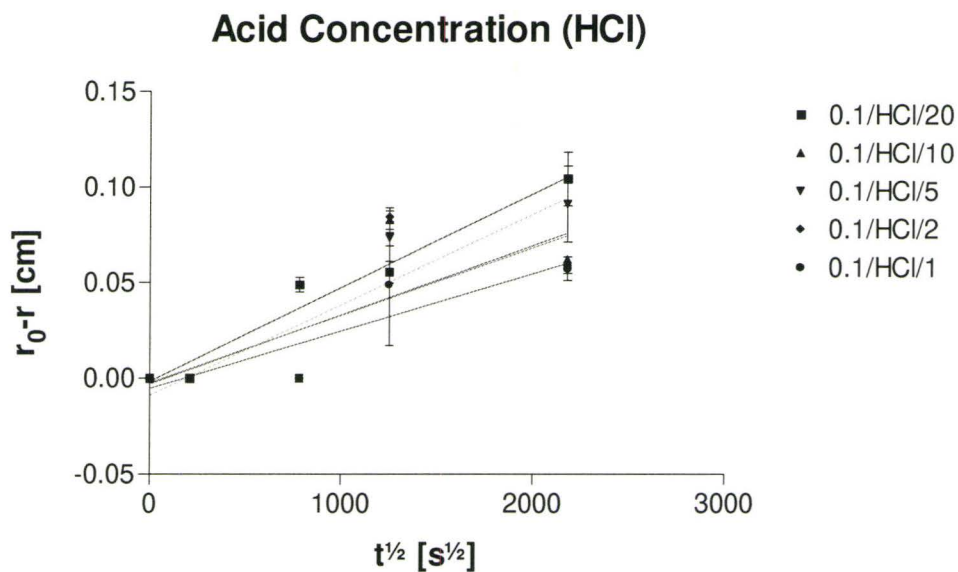


Figure 22. Diffusion rate at different concentrations of hydrochloric acid.

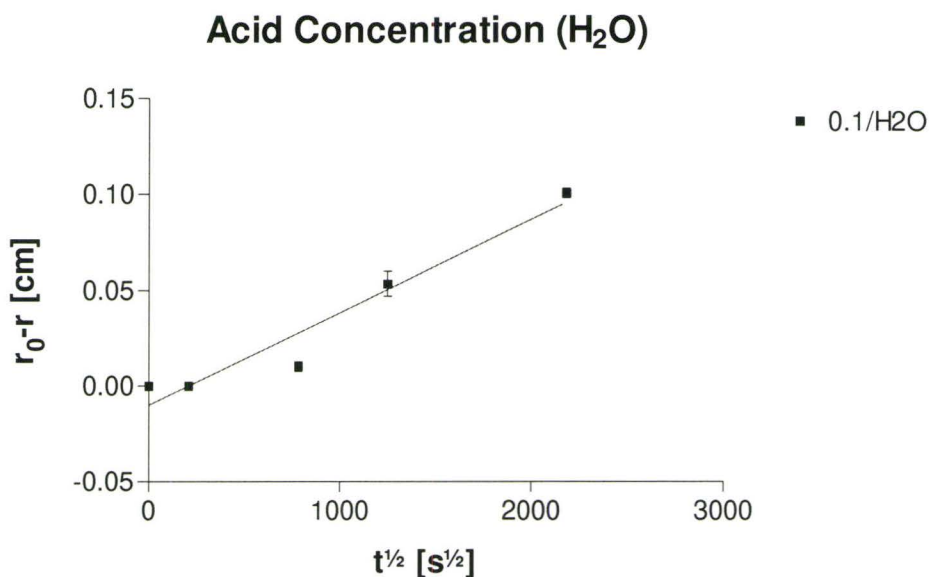


Figure 23. Diffusion rate in water.

3.2.3 Indicator concentrations:

As the indicator concentration increases within the composite, the indicator seems to increase in distribution throughout the polymer matrix. The following figures (Figure 24a & 25a) are x-ray mapped images of the original SEM micrograph (Figure 24b & Figure 25b). In which the x-ray signals of sodium and oxygen appear to be in a high concentration in one specific area as is the case in Figure 24a. Yet the signals are dispersed throughout the image (Figure 25a), which suggests that the indicator is more distributed at higher concentrations.

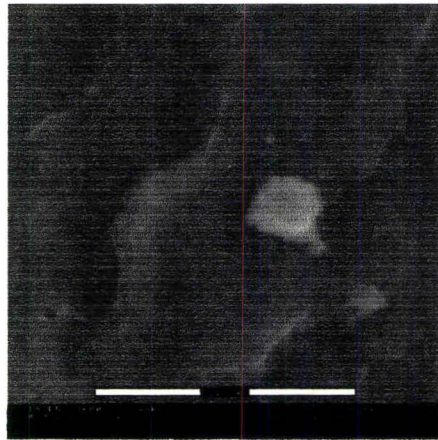
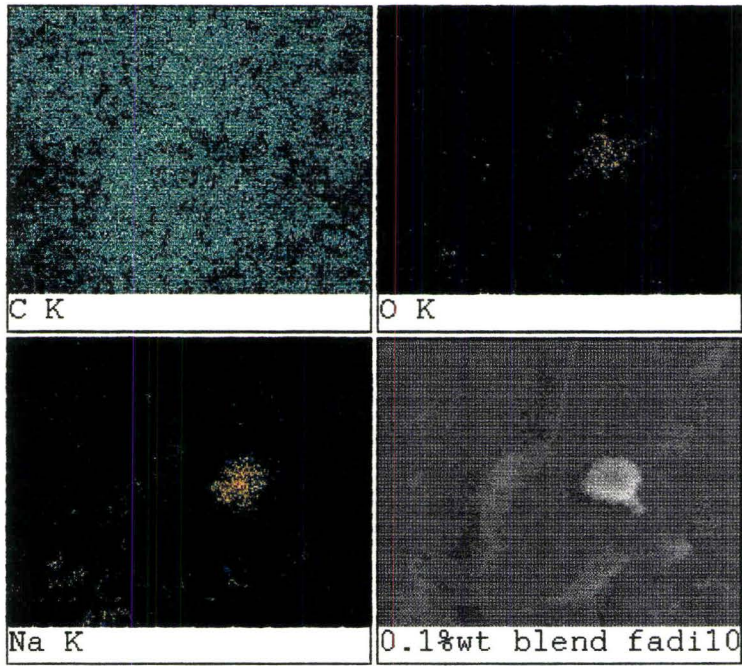


Figure 24. SEM micrograph 0.1%wt indicator composite.

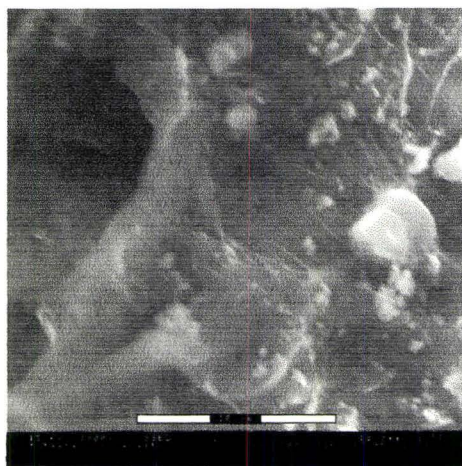
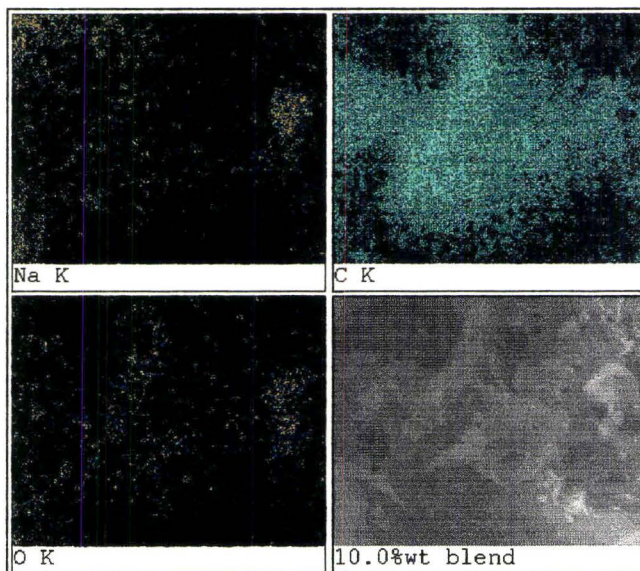


Figure 25. SEM micrograph 10.0%wt indicator composite.

The increased concentration of the indicator causes the apparent decolorization rate to decrease dramatically (Figures 26, 27 & 28). This decrease indicates that a higher concentration of acid is needed to diffuse into the polymer matrix at higher indicator concentrations. A mechanism for diffusion may be proposed based on this data. There are two general mechanisms of diffusion: i) site to site hopping and ii) diffusion along a long lived pathway in the polymer matrix. The first mechanism describes the diffusing molecule hopping from a void within the polymer matrix to another void, where the voids are created by the segmental chain motion and are short lived. The second mechanism describes the diffusing molecule moving along some pathway into the polymer matrix, where the pathway is created by long lived voids between the polymer chains. With regards to these composites, an observation of a dramatic increase in the decolorization rate with an increase of indicator loading, would indicate the second mechanism. This would be due to the connectivity of the indicator domains which would create a long lived "void" with respect to the surrounding polymer chains. Yet this is not the case, which gives support to the idea of a site to site hopping mechanism for the diffusion process. The polar domains seem to increase in size and distribution, yet based on the SEM micrographs, no conclusion can be ascertained on the connectivity between the domains. It must be noted that the diffusion of the acid should be constant. If this value does change as the indicator concentration changes then there must be a change in the diffusion mechanism.

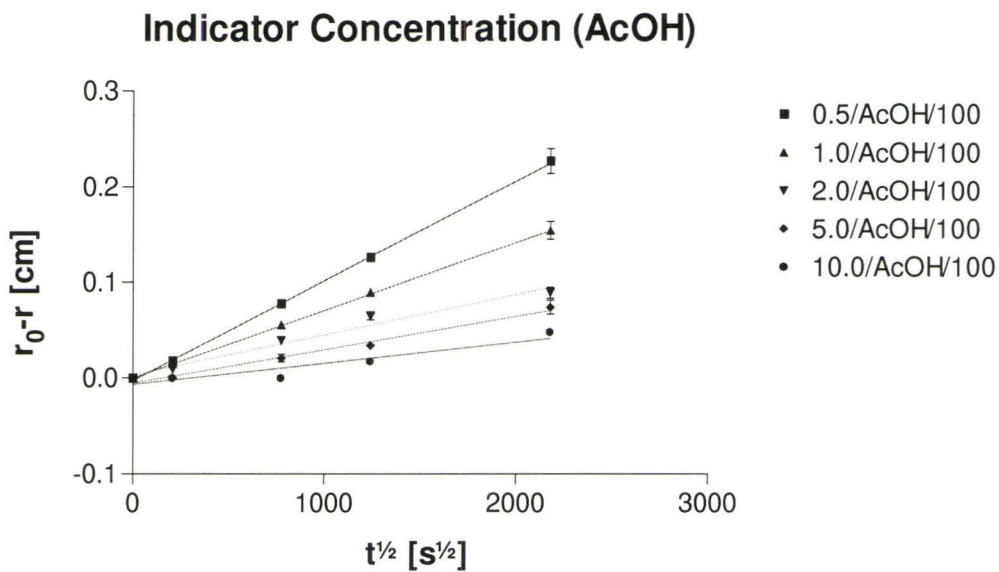


Figure 26. Diffusion rate at different loadings in acetic acid.

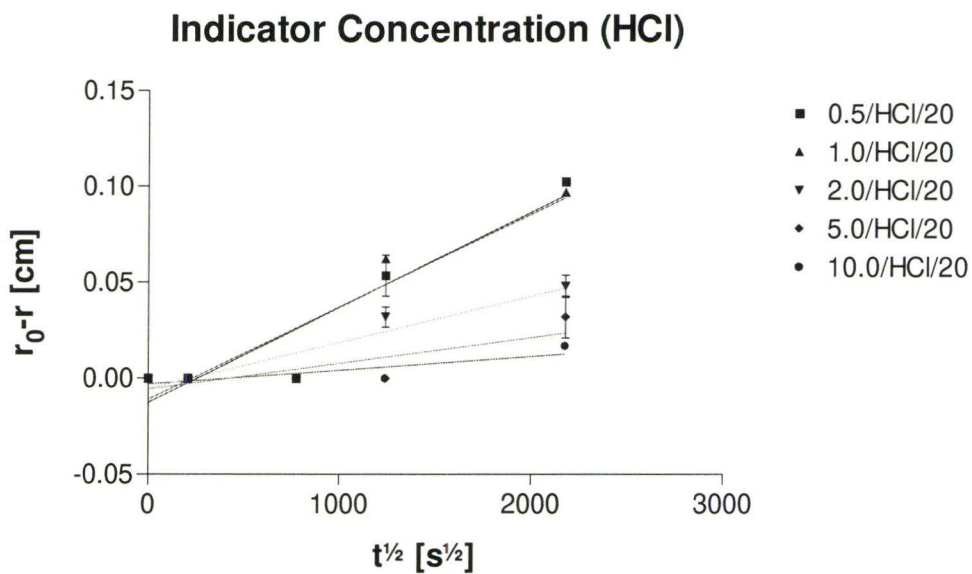


Figure 27. Diffusion rate at different loadings in hydrochloric acid.

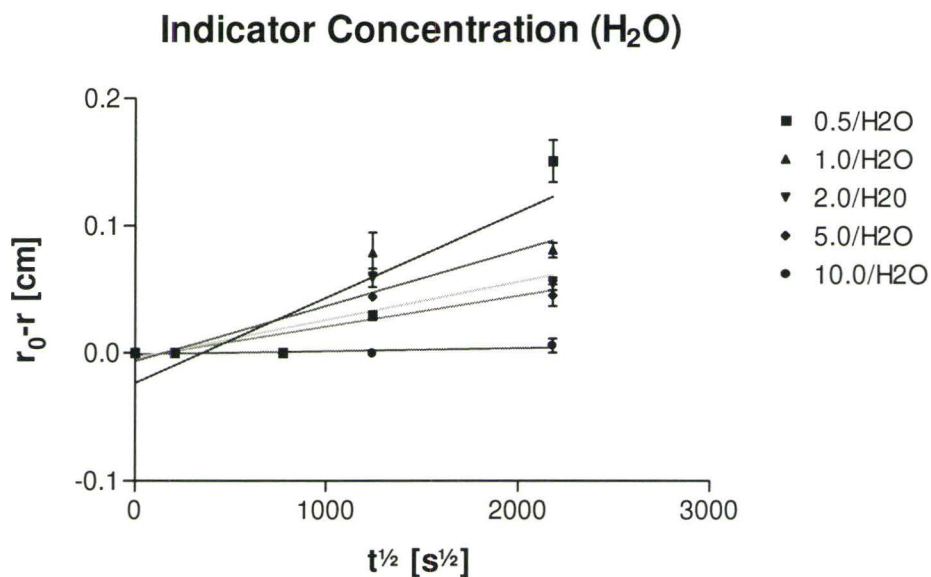
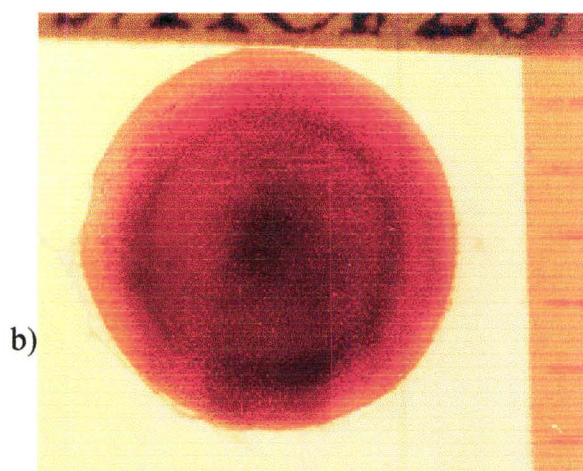
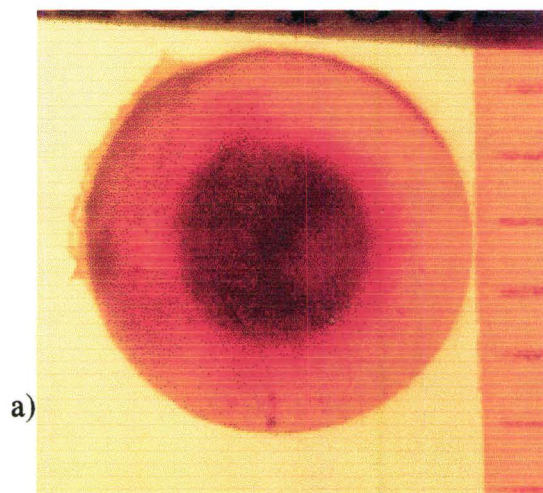


Figure 28. Diffusion rate at different loadings in water

An additional observation that indicates the rate of diffusion of the acids is in the nature of the decolorization. The following figure is a sample of the cross sections of a 0.5wt% indicator composite exposed to water (Figure 29a), hydrochloric acid (Figure 29b) and acetic acid (Figure 29c).



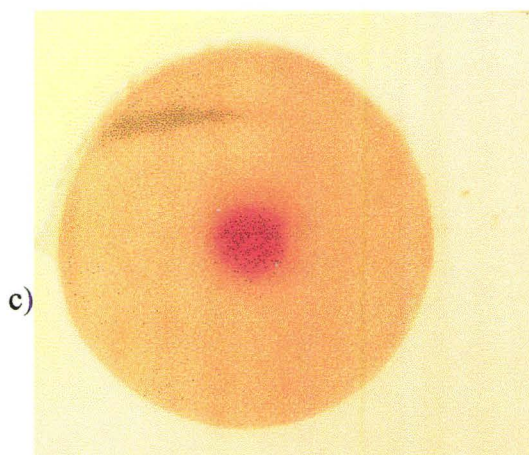


Figure 29. Decolorization of 0.5%wt indicator composite in a) water, b) hydrochloric acid and c) acetic acid.

Between the three samples, Figure 29c appears to have the most distinct color boundary, as opposed to the color gradient apparent in the other cross sections. A sharp color boundary is indicative of rapid diffusion of acid, whereas a gradient of color as a boundary is indicative of slow diffusion of acid. This observation supports the data which indicate that the diffusion rate of acetic acid is greater than that of water or hydrochloric acid.

3.3 Diffusion:

3.3.1 Diffusion Model:

The diffusion of acids into a polymer matrix such as polyethylene is dependent on concentration of the diffusing molecule. With respect to the diffusing molecule in these experiments, diffusion is apparently dependent on both the concentration of the acid and its polarity. The following are the possible methods of estimating the diffusion coefficient.

The easiest mold to make was that of a cylinder, which facilitates the use of "The cylindrical diffusion model". This assumes that the cylinder is infinitely long and circular in which diffusion is radial everywhere. In terms of the dimensions of the experimental cylinders, they must have a large aspect ratio (Length/Diameter) in order to use this model. The equation for radial flow in a cylinder, where the initial conditions are i) a circular cylinder of radius r is the diffusion medium, ii) a constant concentration is maintained at its surface, and iii) the medium is initially free of solute. The solution of the model with the aforementioned conditions is as follows in terms of Bessel's functions:³⁷

$$C = C_0 \left[1 + \frac{2}{a} \sum_{n=1}^{\infty} \frac{1}{\alpha_n} \frac{J_0(r\alpha_n)}{J_1(a\alpha_n)} e^{-D\alpha_n^2 t} \right] \quad (7)$$

where α is the root of a Bessel function of the zero order, J_0 and J_1 are Bessel's functions of zero order and first order respectively, r is the radius at time t , a is the original radius and C_0 is the constant concentration at the surface of the cylinder. This equation describes the concentration gradient throughout the cylinder. However, since both the diffusion coefficient and the exact concentration at a given radius are unknown, this equation cannot be applied to this system, a simpler model is needed based on the observables, which is the change in colored radii.

It is first assumed that at the diffusional front a finite boundary exists between the unreacted and the fully protonated region (Figure 31). For this to be established, it is assumed that the radial diffusion of the acid must be uniform and the area of the singly protonated indicator be very small. Based on these assumptions, the concentration of the acid at the boundary is twice the concentration of the indicator in the matrix and is always constant. Since the radial diffusion is uniform along the circumference of the circle, then at the

molecular level, the cylinder can be treated as a plane, allowing the calculation of the plane diffusion (Figure 30), which will allow for the approximation of the radial diffusion.

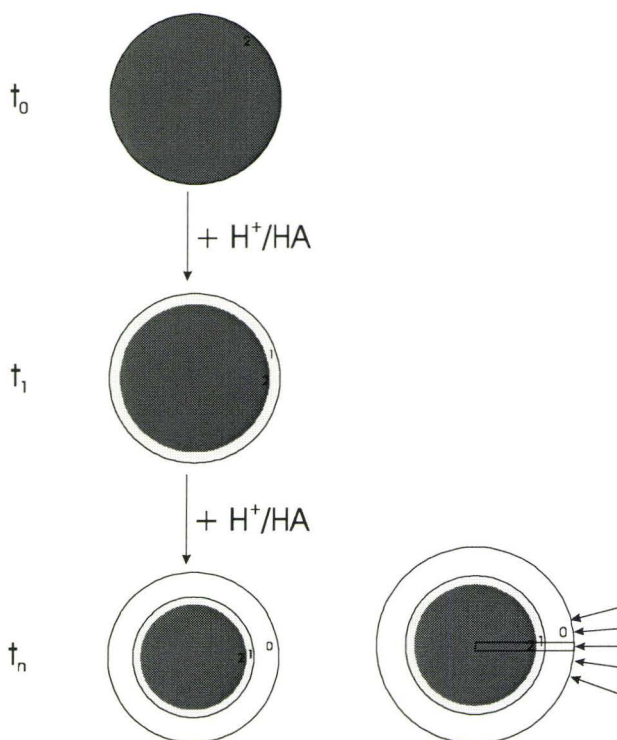


Figure 30. Diagram of diffusion front and plate approximation.

The equation for the plane diffusion is as follows:

$$C = C_0 \operatorname{erfc} \left(\frac{x}{2\sqrt{Dt}} \right) \quad (8)$$

where C is the concentration of the diffusant, which is twice the concentration of indicator. C_0 is the original concentration of the diffusant outside the diffusion medium. x is the distance the diffusing species has moved with respect to time t , and D is the diffusion coefficient. $\operatorname{erfc}[x/2(Dt)^{1/2}]$ is the error-function complement defined as follows:

$$\operatorname{erfc}(z) = 1 - \frac{2}{\pi} \int_0^z e^{-\eta^2} d\eta \quad (9)$$

where $\eta = \frac{x}{2\sqrt{Dt}}$, and z is some value. $\operatorname{erfc}(z)$ is a constant value for a given z and the solutions to this function can be found in standard mathematical tables.

Since C/C_0 is constant at any given time then:

$$\frac{C}{C_0} = \operatorname{erfc}\left(\frac{x}{2\sqrt{Dt}}\right) = \operatorname{erfc}(\eta) \quad (10)$$

Now the diffusion coefficient can be calculated as follows:

$$x = (\sqrt{D} 2 \eta) \sqrt{t} \quad (11)$$

$$D = \left(\frac{\text{slope}}{2 \eta}\right)^2 \quad (12)$$

The slopes of all the curves plotted can be used in **12**. However, it must be noted that this diffusion coefficient is an empirical value, since the concentration of acid is estimated rather than measured directly and that the consumption of the diffusin acid by the indicator, is not accounted for in the existing model. In principle, one could eliminate this latter effect by extrapolating the observed diffusion coefficients to zero indicator loading. It must be further verified by comparing these values to the values obtained from the cylindrical model

based on the exact concentration of the acid at a given time.

3.3.2 Experimental diffusion coefficients:

With the naked eye, there is an apparent finite boundary, but inspection under the optical microscope reveals a color gradient between the unreacted region and the reacted region. The boundary is defined as the line that distinguishes between the darkest region of the cross-section and the rest (Figure 31).

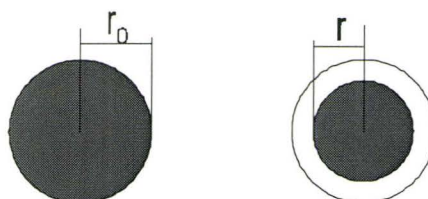


Figure 31. Diagram of acid front.

The values obtained for the empirical diffusion coefficient D_e and the diffusion rate R_D at different conditions, are tabulated in the following tables.

Sample	R_D [cm/s ^{1/2}]	D_e [cm ² /s]
0.1/AcOH/100	1.32E-04	6.68E-10
0.1/AcOH/50	1.30E-04	7.19E-10
0.1/AcOH/10	3.70E-05	7.80E-11
0.1/AcOH/5	4.70E-05	1.47E-10
0.1/AcOH/2	2.80E-05	6.66E-11
0.1/AcOH/1	4.00E-05	1.71E-10

Table 5. D_e and R_D for 0.1/AcOH data series.

Sample	R_D [cm/s ^{1/2}]	D_e [cm ² /s]
0.1/HCl/20	4.90E-05	9.98E-11
0.1/HCl/10	3.50E-05	5.96E-11
0.1/HCl/5	4.70E-05	1.15E-10
0.1/HCl/2	3.50E-05	7.36E-11
0.1/HCl/1	3.00E-05	8.23E-11

Table 6. D_e and R_D for 0.1/HCl data series.

Sample	R_D [cm/s ^{1/2}]	D_e [cm ² /s]
0.1/H ₂ O	4.90E-05	7.89E-11

Table 7. D_e and R_D for 0.1/H₂O data.

Sample	R_D [cm/s ^{1/2}]	D_e [cm ² /s]
0.5/AcOH/100	1.05E-04	3.82E-10
1.0/AcOH/100	7.10E-05	2.86E-10
2.0/AcOH/100	4.20E-05	1.17E-10
5.0/AcOH/100	3.50E-05	1.03E-10
10.0/AcOH/100	2.20E-05	5.20E-11

Table 8. D_e and R_D for indicator concentration (AcOH) data series.

Sample	R_D [cm/s ^{1/2}]	D_e [cm ² /s]
0.5/HCl/20	5.00E-05	9.32E-11
1.0/HCl/20	4.80E-05	1.47E-10
2.0/HCl/20	2.40E-05	4.38E-11
5.0/HCl/20	1.40E-05	1.97E-11
10.0/HCl/20	7.00E-06	6.57E-12

Table 9. D_e and R_D for indicator concentration (HCl) data series.

Sample	R_D [cm/s ^{1/2}]	D_e [cm ² /s]
0.5/H ₂ O	6.70E-05	1.35E-10
1.0/H ₂ O	4.40E-05	8.85E-11
2.0/H ₂ O	3.00E-05	4.66E-11
5.0/H ₂ O	2.40E-05	3.60E-11
10.0/H ₂ O	2.00E-06	2.99E-13

Table 10. D_e and R_D for indicator concentration (H₂O) data series.

All the values for R_D were obtained by a linear regression of their respective plots. Table 5 shows the fastest rate, which is apparent when the acid used is glacial acetic acid and 50% acetic acid at an indicator concentration of 0.1%wt (this rate decreases as the acetic acid concentration decreases). There is no apparent pattern exhibited by the hydrochloric acid set, however comparison of the acetic acid, hydrochloric acid and water sets suggests that the non-dissociated acid is more efficient in decolorizing than ionic acids or water. At this point, it is assumed that the non-dissociated acid (acetic acid) can diffuse faster into the nonpolar matrix than ionic acids (H⁺/Cl⁻). In the sets where the indicator concentration is modified, the same phenomenon is observed, the more the indicator concentration the slower the rate. Intuitively the higher the indicator concentration the more

acid that is need to diffuse into the polymer matrix, thereby slowing down the rate of decolorization, as observed in Tables 8, 9 and 10.

According to literature¹, the diffusion coefficient for water in LDPE at 25°C ranges from 10^{-8} to 10^{-7} cm²/s. It is suggested that the diffusion coefficient for HDPE would be less that that of LDPE, because of the increased crystallinity in HDPE. Likewise, LLDPE has an increased crystallinity, although they would be comparable.

Willet, reports diffusion coefficients for water into polyethylene/starch composites on the order of 10^{-10} to 10^{-11} cm²/s for LDPE. The decrease in the diffusion coefficient is attributed to the increase in starch loading which leads to greater crystallinity of the composite; this amounts to a decrease in the diffusion rate.

Likewise, in these LLDPE/phenolphthalein disodium composites, a decrease is observed in the diffusion coefficient for water with respect to the indicator loading. However, the reason for this is not clear, it could be attributed to the increased crystallinity of the composite, or due to the increased need for acid to protonate the indicator.

The following are graphs (Figures 32,33 & 34) of the diffusion coefficients as a function of indicator concentration. These graphs are needed in order to establish a diffusion coefficient for the acids at zero indicator loading.

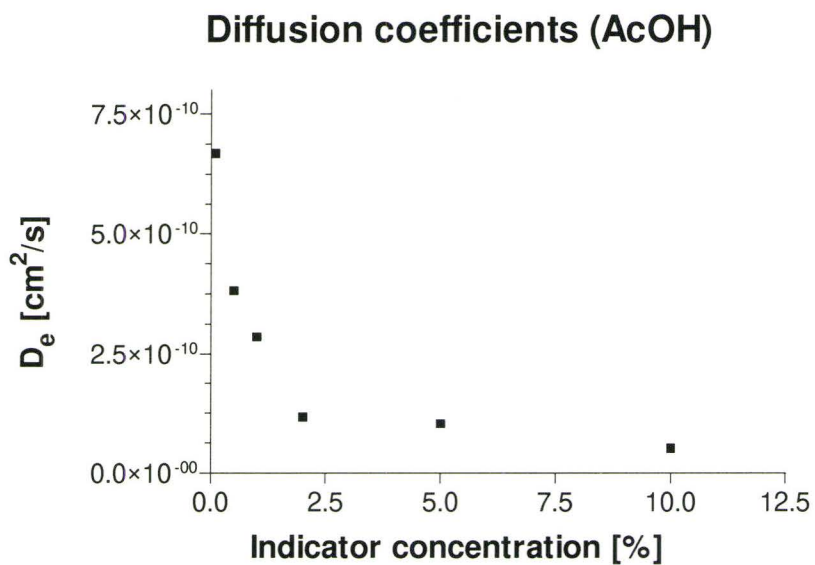


Figure 32. Graph of diffusion coefficients in acetic acid

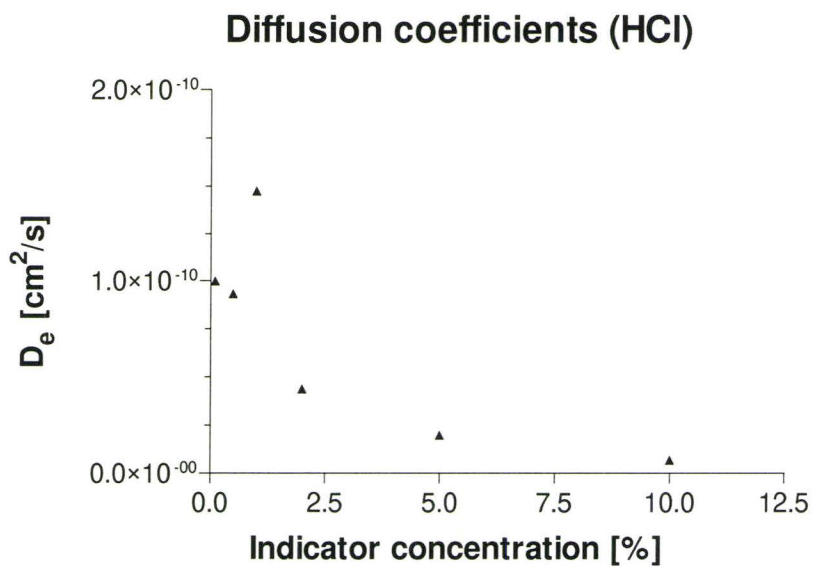


Figure 33. Graph of diffusion coefficients in hydrochloric acid.

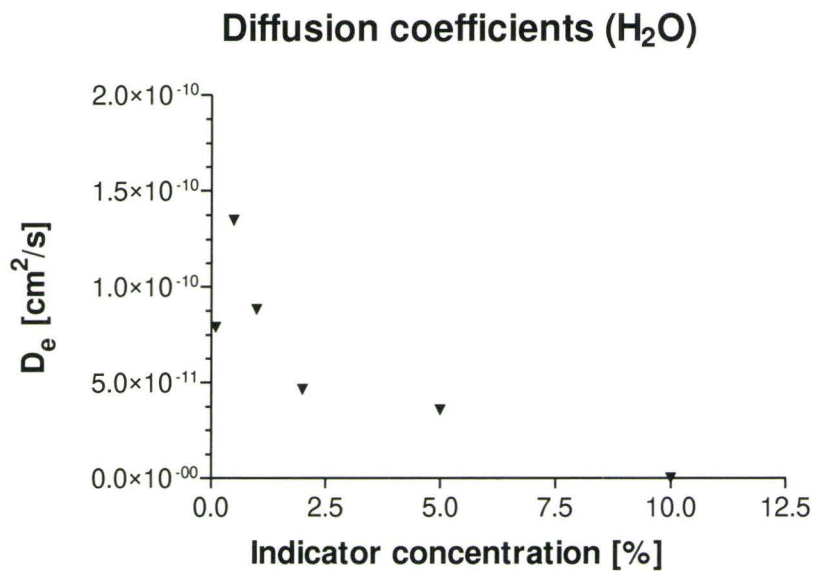


Figure 34. Graph of diffusion coefficients in water.

However, it is observed that the graphs do not follow a linear trend, particularly Figure 32 (acetic acid). This seems to indicate the curves are composed of two linear regions. It is not clear what this means or why this is so.

4.0 Conclusions:

A polymer composite has been made to respond to acidic media by a change in color. The aspects of the composite investigated were:

- a) The effect of different acids and the selectivity of the composite in terms of acid polarity or acid strength. It was observed that acetic acid caused a faster decolorization than hydrochloric acid or water. However, as the concentration of acetic acid was decreased the decolorization slow down. This strongly suggests that the acidic species that diffuses into the composite is the non-dissociated acid (acetic acid), rather than the ionic acids (H^+/H_3O^+). In this sense the composite is selective between acids with low dissociation constants and acids with high dissociation constants.
- b) Proposing a diffusion mechanism for the decolorization. It is known theoretically and experimentally that the diffusion mechanism for polymers such as polyethylene is that of a site-to-site hopping mechanism. The mechanism for decolorization would involve a non-dissociated acid diffusing into the matrix by hopping from site to site, until encountering an indicator domain or molecule, where it reacts with and renders the indicator colorless.
- c) Exploring the use of these composites to measure diffusion coefficients. The diffusion model proposed is based on the following assumptions i) The diffusion of the acid is uniform around and throughout the composite cylinder, ii) The

concentration of the monoprotonated indicator species is low enough to be negligible, and iii) the concentration at the boundary is constant. This model does not account for any acid that diffuses into the matrix and does not react with the indicator, or for the fact the acid is consumed by the indicator as it diffuses into the composite. However, diffusion coefficients can be calculated for these composites. They are empirical by nature, but viable since they are reasonable and comparable to the data reported in the literature.

- d) Exploring its use as long term acid meters. In principle, any indicator or mixture of indicators can be incorporated in a similar matrix. The process of decolorization is diffusion limited, allowing for its use as a long term monitor of acids within a system.

Other conclusions that were arrived at through investigating the production process of the composite are as follows:

- a) The parameters that effect the decolorization of the composite with regards to extrusion are, i) the concentration of indicator, which is an inverse relationship, and ii) the rate of mixing, which is a direct relationship to the apparent diffusion rates.
- b) An attempt to modify the indicator to increase the dispersion of the indicator within the polymer was made by the addition of ethylene glycol. It was found that a 1:1 ethylene glycol to phenolphthalein disodium mixture could afford a better dispersion. This means that the system within the extruder can be switched from a liquid-solid system to a liquid-liquid system.

5.0 Future Work:

These are the major aspects that require further investigation:

1. The measurement of the actual concentration of acid within the composite cylinders at a given time. This is a requirement for the use of the cylindrical model proposed to calculate the diffusion coefficients. These will be compared to the empirical diffusion coefficients to substantiate the results. Several techniques could be utilized to do so. One of the techniques that has been used and studied extensively is the use of NMR.⁴⁷⁻⁴⁹
2. The nature of the interface between the indicator and the polymer matrix. This investigation would help understand the nature of the dispersion of indicator within the polymer matrix, which may help in enhancing the resolution of the color boundary. This includes the study of the dispersion process within the extruder, the effect of dispersion of the indicator on the decolorizing process.
3. This system can be viewed from the perspective of an ion-exchange resin, where protons are exchanged for sodium cations. In order to verify this, identification of the diffusing species and exploring why decolorization occurs in the presence of water is necessary. This may be done by examining the sample solutions after decolorization, either by pH monitoring, UV/Vis spectroscopy or monitoring with a sodium selective electrode, in an attempt to identify any species diffusing out of the composite.

4. Comparison of acids such as propionic and butyric acid, as well as other aqueous acids with different acid strengths. To investigate the relationships between the compatibility of the acid with the polymer matrix, versus acid strength.

6.0 Appendix I: Standard NMR data

Phenolphthalein; 3,3-Bis(p-Hydroxyphenyl)-phthalide

MW:318.089

Sadtler Standard Carbon-13 NMR Spectra; CNM2 4959, IR 02040

SO: CDCL₃/DMSO-D IN: VAR. CFT-20 CO: 0. ppm D T :

05.03.81

ST: TMS

TE: 309K

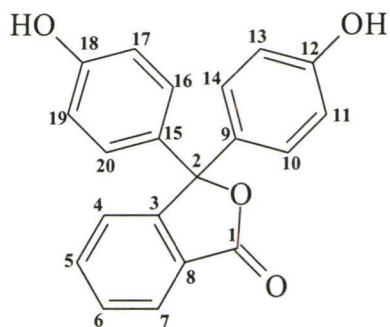
OR: SAD04455

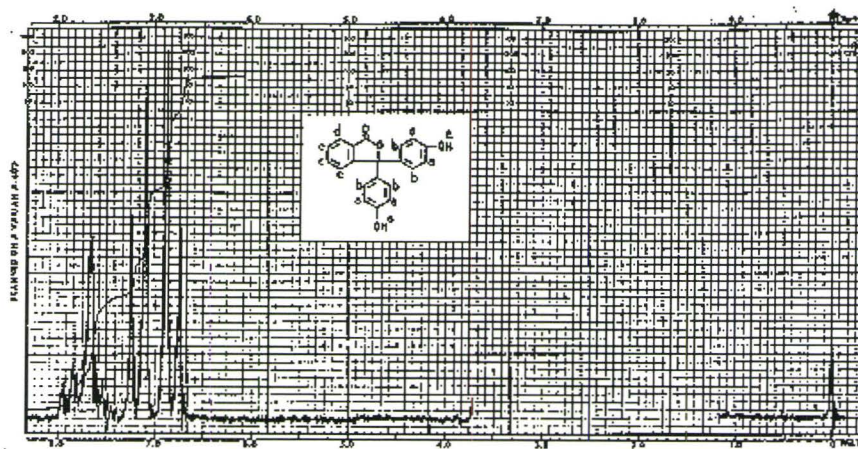
QU: 91

Chemical Shifts(ppm), Multiplicity:

1	169.30 -	6	125.00 -	11	115.20-	16	128.20-
2	91.70 -	7	129.00 -	12	157.60-	17	115.20-
3	152.80 -	8	125.20 -	13	115.20-	18	157.60-
4	124.10 -	9	131.30 -	14	128.20-	19	115.20-
5	134.10 -	10	128.20 -	15	131.30-	20	128.20-

<S 14709>





14709 M

PHENOLPHTHALEIN

IR 8113

 $C_{20}H_{14}O_4$ Mol. Wt. 318.33Source: E. Merck AG
Darmstadt, Germany

Filter bandwidth:	4	Hz
Sweep time:	250	sec
Sweep width:	500	Hz
Sweep offset:	-	Hz
Spectrum amp:	40	Hz
Integral amp:	80 (spec. amp. 6.3)	
Solvent:	Dimethyl sulfoxide at 70°C	

ASSIGNMENTS

a	6.81	h	_____
b	7.14	i	_____
c	7.35-7.80	j	_____
d	7.88	k	_____
e	unobserved	l	_____
f	_____	m	_____
g	_____	n	_____

Sadler Standard 1H NMR Spectrum of Phenolphthalein.

40196M

PHENOLPHTHALEIN, DISODIUM SALT

 $C_{20}H_{12}Na_2O_4$

Mol. Wt. 362.30

PRISM NO.

67246

Source of Sample:

Tokyo Kasei Kogyo Company Ltd.,
Tokyo, Japan

SOLVENT

 D_2O

REFERENCE

TSP

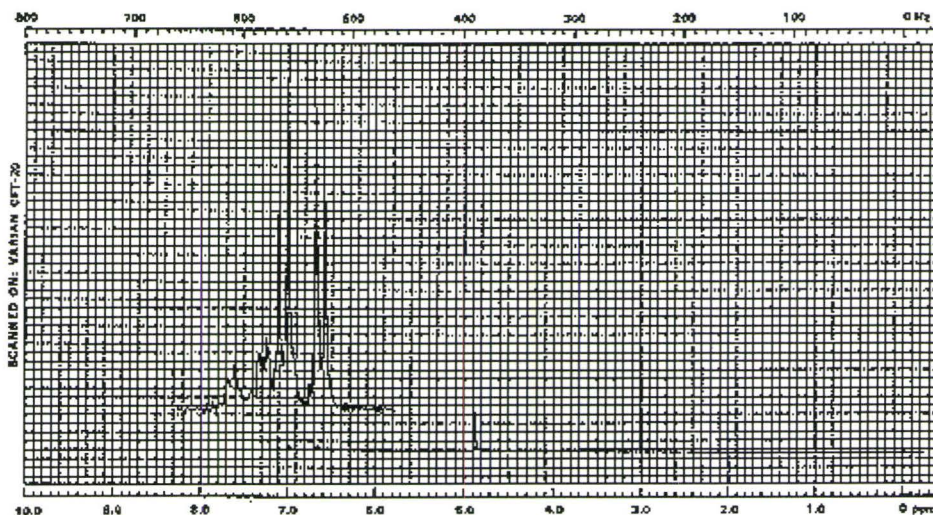
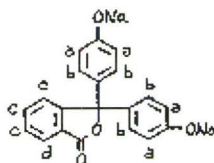
SWEEP OFFSET

"

NMR © 1985 Sadtler Research Laboratories, Division of Bio-Rad Laboratories, Inc.

ASSIGNMENTS

a	6.65	f	_____	k	_____	p	_____
b	7.04	g	_____	l	_____	q	_____
c	6.80-7.50	h	_____	m	_____	r	_____
d	7.64	i	_____	n	_____	s	_____
e	4.88 H ₂ O	j	_____	o	_____	t	_____

Sadtler Standard 1H NMR Spectrum of Phenolphthalein disodium salt.

7.0 Appendix II: Extrusion

The design of the single screw extruder provides for the circulatory motion of the polymer in the channel, leading to good laminar mixing and narrow residence time distribution. This is depicted in the diagram below:

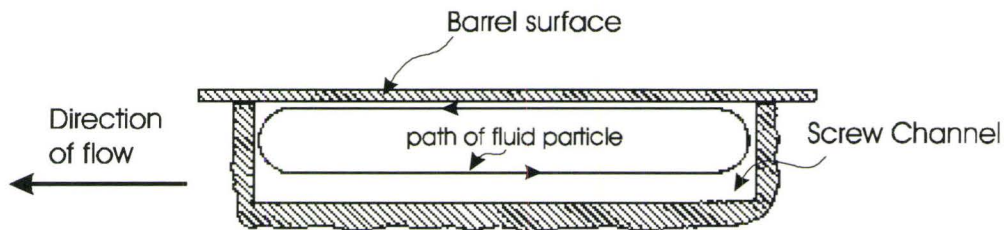


Figure A-1. Diagram of melt flow in a single-screw extruder

The laminar mixing within between each flight, where circulation occurs as the melt plug moves forward. The narrow residence time distribution, is the distribution of the time taken for a fluid particle to move within the melt circulating between the flights of the screw. To have a narrow residence time distribution requires that an efficient circulation of the polymer melt within the channels exist. This leads to efficient mixing of the material and good laminar mixing.

The following parts are to introduce the reader to different types of mixers.

Batch mixers:

Batch mixers are the oldest type yet very versatile units that are still widely used today. The operating conditions can be varied during the cycle, additives can be added at an optimal time sequence, and temperature can be controlled. There are three kinds of batch mixers: i) particulate solids mixers, ii) extensive liquid mixers, and iii) intensive liquid

mixers. They are classified based on their application and the nature of the primary mixing mechanism. Particulate solids mixers, also referred to as blenders, involve generally a random distributive mixing mechanism. On the basis of their operation, they can be a “tumbling” type, “agitating ribbon”, or “fluidized bed” mixers. The tumbling type mixers are the simplest mixers, however they cannot handle difficult mixtures. It tends to segregate and cannot handle sticky material due to the tumbling action that occurs, a build up of electrostatic charge is acquired. However, the latter property can be an advantage, with the blending of dry pigments with nonpolar polymers, or during the mixing of two components with opposite electric charges. Ribbon blenders are useful with sticky mixtures, but requires more power than the tumbling mixers. These mixers generates a considerable electrostatic charge. Fluidized bed mixers are rapid mixers that cannot deal with sticky powders or powder mixtures with pronounced density and shape variations which would lead to segregation problems. This mixer does generate a small electrostatic charge.

Liquid mixers are dominated by laminar mixing mechanisms and bring about an increase in the interfacial area between the components, and the distribution of interfacial elements throughout the mixer volume. There are low and high viscosity mixers, with the low viscosity mixers operating in the viscosity range of 0.5 - 500 Ns/m². Examples of these mixers are the impeller-type mixers and the high speed dispersion mixers. Turbulent mixing plays a significant role in these mixers. The high viscosity mixers impart extensive mixing and are characterized by high shear stress zones where dispersive mixing and homogenization take place. These mixers are used extensively in the elastomer and plastics industry.

Continuous mixers:

The advantages of continuous mixing are that it has a large output, uninterrupted operation, greater product uniformity, easier quality control and reduced manpower. The

disadvantages would include the generation of lower dispersive mixing quality and possess less flexibility in switching to new mixtures. Therefore the single screw and twin screw extruders have been modified to incorporate into the design, mixing devices to improve temperature uniformity and mixing.

8.0 References:

1. J.L. Willett, *Polym Eng. Sci.*, **35**(14), 1184 (1995)
2. B.K. Jasberg, C.L. Swanson, R.L. Shogren, and W.M. Doane, *J. Polym. Mater.*, **9**, 163 (1992)
3. J.S. Peansky, J.M. Long, and R.P. Wool, *J. Polym. Sci. Polym. Phys. Ed.*, **29**, 565 (1991)
4. Principles of Polymer Systems, F. Rodriguez, Hemisphere Publishing Corp, New York, 1989.
5. Composite Materials: Science and Engineering, K. K. Chawla, Springer-Verlag, New York, 1987
6. R. Fayt , R. Jérôme and Ph. Teyssié, *J. Polym. Sci., Polym. Phys.*, **27**, 75-793 (1989)
7. R. Fayt , R. Jérôme and Ph. Teyssié, *Polym. Eng. Sci.*, **27**, 328-334 (1987)
8. R. Fayt, R. Jérôme and Ph. Teyssié, *Makromol. Chem.*, **187**, 837-852 (1986a)
9. R. Fayt , R. Jérôme and Ph. Teyssié, *J. Polym. Sci., Polym. Lett.* **24**, 25-28 (1986b)
10. W.E. Baker and M. Saleem, *Polymer*, **28**, 2057-2062 (1987)
11. S.Y. Hobbs, R. C. Bopp and V. H. Watkins, *Polym. Eng. Sci.*, **26**, 517-524 (1986)
12. H.P. Grace, *Chem. Eng. Commun.*, **14**, 225-277 (1982)
13. J.M. Willis, and B. D. Favis, *Polym. Eng. Sci.*, **28**, 1416-1426 (1988)
14. G. I. Taylor, *Proc. Roy. Soc.*, **A146**, 41 (1932)
15. W. R. Bolen and R. E. Colwell, *Soc. Plast. Eng. J.*, **14**(8), 24-28 (1958)
16. R.B. Bird, H.R. Warner, Jr. and D.C. Evans, *Fortsch. Hochpolymerenforch.*, Springer-Verlag, Berlin, **8**, 1-90 (1971)
17. A. Baeyer, *Ber. D. Chem. Ges.* **4**, 658 (1871)

18. M.H. Hubacher, U.S. Patent 1 940 494 Dec. 19; C.A., **28**, 1366
19. Ex-Lax Co. Brit. Patent 532 045, Jan 16, 1941; C.A., **36**, 498
20. Z. Von Vámosy, First "Purgen" ein schädliches Abführmittel? Munch. Med. Wochenschr., 50: 1124-1126, 1908
21. E. Y. Grantscharova, I. A. Avramov, I. S. Gutzow, *Comptes Rendus de L Acadmie Bulgare des Sciences*, **37**(11), 1521 (1984)
22. E. Ziegler and H. Sterk, *Monatsh. Chem.*, **100**, 1604-1607 (1969)
23. S. Berger, *Tetrahedron*, **37** 1607-1611 (1981)
24. Z. Tamura, S. Abe, K. Ito and M. Maeda, *Anal. Sci.*, **12**, 927 (1996)
25. R. Hagen and J. D. Roberts, *J. Am. Chem. Soc.*, **91**, 4504 (1969)
26. G. Schwarzenbach and O. Hagger, *Helv. Chim. Acta*, **20**, 1591 (1971)
27. M. Buu-Hoi, *Bull. Soc. Chim*, **8**(5), 165 (1941)
28. Flieg, *Chimisches Zentralblatt*, **II**, 363 (1909)
29. H. Schonhorn, H.L. Frisch, R.V. Albarino, *J. Polym. Sci. Polym. Phys. Ed.*, **11**, 1013 (1973)
30. A. Keller, *Philos. Mag.*, **2**, 1171 (1975), *Prog. Phys.*, **31**, 623 (1968)
31. K. Bergmann, K. Naworki, *Kolloid Z.*, **219**, 132 (1957)
32. S.-D. Clas, D.C. McFaddin, K.E. Russell, *J. Polym Sci Part B*, **25**, 1057 (1987)
33. R.S. Stein, R. Prud'homme, *J. Polym. Sci Part B*, **9**, 595 (1971)
34. *Polymer Processing: Principles and Design*, D.G. Baird and D.I. Collias, Butterworth-Heinemann, Toronto (1995)
35. E. Y. Grantscharova, I. A. Avramov, I. S. Gutzow, *Comptes rendus de l'Académie bulgare des Sciences*, **37**(11), 1521 (1984)
36. *Polymer Handbook 3rd ed.*, J. Brandrup, E.H. Immergut eds., John Wiley & Sons, New York 1989

37. *Diffusion In and Through Solids*, R. M. Barrer, University Press, Cambridge, 1951.
38. *Statistics for Experimenters*, G.E.P. Box, W.G. Hunter, J.S. Hunter, John Wiley & Sons, Toronto, 1978
39. *The Merck Index, 11th ed.*, Merck & Co., Inc. Rahway, NJ, 1989
40. *Concise Encyclopedia of Polymer Science and Engineering*, J. I. Kroschwitz, John Wiley & Sons, NY, 1990
41. B.D. Favis, *The Canadian Journal of Chemical Engineering*, **69**, 619 (1991)
42. M. Sumita, T. Ookuma, K. Miyasak and K. Ishikawa, *J. Appl. Polym. Sci.*, **27**, 3059-3066 (1982)
43. J. Kubàt, M. Rigdahl and M. Welander, *J. Appl. Polym. Sci.*, **39**, 1527-1539 (1990)
44. R. Kaliski, A. Galeski and M. Kryszewski, *J. Appl. Polym. Sci.*, **26**, 4047-4058 (1981)
45. R.L. Evangelista, Z.L. Nikolov, W. Sunq, J.-L. Jane and R.J. Gelina, *Ind. Eng. Chem. Res.*, **30**, 1841 (1991)
46. *Diffusion in Polymers*, P. Neogi, Marcel Dekker Inc., New York, 1996
47. M. Ercken, P. Adriaensens, D. Vanderzande and J. Gelan, *Macromolecules*, **28**, 8541-8547 (1995)
48. A.G. Webb and L.D. Hall, *Polymer*, **32**, 2926 (1991)
49. H.L. Frisch, *Polym. Eng. Sci.*, **20**, 2 (1980)